Inter-Cell and Intra-cell Interference Coordination in Cellular Network with Highly-Sectored Base Stations

by

Heba Eid
B. Sc. in Communication Engineering

A thesis submitted to the
Faculty of Graduate Studies and Research
in partial fulfillment of the requirements for the degree of

Master of Applied Science in Electrical and Computer Engineering

Ottawa-Carleton Institute for Electrical and Computer Engineering
Department of Systems and Computer Engineering
Carleton University
Ottawa, Ontario
May 2011

The undersigned hereby recommend to
the Faculty of Graduate Studies and Research
acceptance of the thesis

Inter-Cell and Intra-cell Interference Coordination in Cellular Network with Highly-Sectored Base Stations

submitted by

Heba Eid

in partial fulfillment of the requirements for the degree of

Master of Applied Science in Electrical and Computer Engineering

.....

Professor Halim Yanikomeroglu
Thesis Supervisor

.....

Professor Howard M. Schwartz
Chair, Department of Systems and Computer Engineering

Carleton University
May 2011

Abstract

The ever increasing demand on mobile service providers to support high rate applications has prompted the development of OFDM based 4G networks. To meet the rising demand, aggressive reuse of the frequency spectrum and the use of smaller cell sizes will be implemented. This will result in an increase in the interference levels in multi-cell OFDMA networks, especially inter-cell interference. Inter-cell interference can severely degrade system throughput, particularly for cell-edge users.

To counter the effects of inter-cell interference, interference mitigation techniques are used and one of those techniques is inter-cell interference coordination (ICIC). ICIC can be regarded as a form of CoMP (Coordinated Multi-point Transmission) and it is used to collectively schedule transmissions among several base stations to manage the level of interference in the network.

In this thesis, we tackle the inter-cell interference problem by means of an ICIC radio resource scheduling algorithm that aims to improve the cell-edge performance without degrading the overall cell throughput. Conventional scheduling schemes aim to maximize the network throughput; such schemes overlook cell-edge users in scheduling who tend to suffer from bad radio conditions. We consider a recently proposed ICIC scheme which integrates the rate deprived (cell-edge) users in the problem formulation; we implement the scheme in a network in a multi-sectored cells with up to 12 sectors per cell. Coordinated scheduling transmission takes place by coordinating transmission internally between sectors within the same base station (intra-cell), and externally, between neighboring base stations (inter-cell). The use of a multi-sectored base station combined with the aggressive frequency reuse generates a lot of interference in the system but with the coordinated scheduling scheme proposed, we were able to see significant improvement to both network and cell-edge throughput.

Acknowledgements

First and foremost, I am thankful to Allah (God) for everything I have and everything I have accomplished in my life. Secondly, my deepest and warmest gratitude goes to Professor Yanikomeroglu, my Supervisor and Mentor. Under your tutelage, I developed and learned a lot, and for this opportunity, I am forever grateful.

The work done here is done in collaboration with Mahmudur Rahman, a PhD student who has spent endless hours of his precious time discussing his previous work and guiding me towards the finish. I very much appreciate your guidance and support. I am extremely grateful and thankful for all the help you provided during my studies. Thank you.

To Dr. Rainer Schoenen, I thank you for the lengthy hours of discussion, your constructive feedback, your patience, and your guidance with my thesis.

My colleagues who have have supported and encouraged me: Dr. Ramy Gohary, Dr. Petar Djukic, Talha Ahmed, Akram Salem Bin Sediq, Dr. Mohamed Rashad Salem, Dr. Ghassan Dahman, Yasser Fouad, Dr. Sebastian Szyszkowicz, Furkan Alaka, Dr. Abdulkareem Adinoyi, Tarik Shehata, Alireza Sharifian and Tariq Ali, my manager at Alcatel-Lucent.

This work was supported in part by Ontario Graduate Scholarship and by Alcatel-Lucent. I thankfully acknowledge their support.

With all the gratitude I can summon, I am thankful for my family: my mother, father, my sisters, Amany and Salwa, and my Aunt Salwa. Thank you for your steadfast support, your trust, and your faith that I can achieve anything I set my heart on. To my room mate, Mozynah, thank you for your support and patience.

All praise is to Allah.

Heba Eid

Ottawa, Ontario, Canada

May 2011

Table of Contents

List of Tables

List of Figures

List of Acronyms

4G	Fourth Generation
AFFR	Adaptive Fractional Frequency Reuse
AMC	Adaptive Modulation and Coding
BS	Base Station
CSI	Channel State Information
CoMP	Coordinated Multi-Point
eNodeB	Enhanced NodeB
FFR	Fractional Frequency Reuse
GSM	Global System for Mobile
IC	Interference Coordination
ICIC	Inter-cell Interference Coordination
ISI	Inter-symbol interference
IMT-Advanced	International Mobile Telecommunication-Advanced
ITU	International Telecommunication Union
LTE	Long Term Evolution
LTE-A	Long Term Evolution-Advanced
MIMO	Multiple Input Multiple Output
OFDM	Orthogonal Frequency Division Multiplexing
OFDMA	Orthogonal Frequency Division Multiple Access
PFR	Partial Frequency Reuse
QAM	Quadrature Amplitude Modulation
QPSK	Quadrature Phase Shift Keying
SCME	Extended Spatial Channel Model
SFR	Soft Frequency Reuse
SINR	Signal to Interference Noise Ratio
UE	User Equipment

List of Symbols

$h_c(t, f)$	Continuous time impulse response
$\eta_p(t)$	Time-varying delay
$\gamma_p(t)$	Complex gain
p	Propagation path
L	Number of propagation paths
r	Ray
p	Propagation paths
$\alpha_{r,p}$	Amplitude of the sinusoidal rays
$V_{r,p}$	Phase of the sinusoidal rays
$\epsilon_{r,p}$	The doppler frequency
M	Total number of complex sinusoidal rays
n	The OFDM block
k	The tone of OFDM block
$H(n, k)$	Sampled frequency response
N	Number of fading samples
τ	Normalized frequency shift
L_D	Distance dependent pathloss in dB
D	Distance separating transmitter and receiver in km
L_p	Penetration loss measured in dB
X_σ	Gaussian random with standard deviation σ to account for shadowing
θ	Angle between direction of interest and boresight
$A(\theta)$	Antenna pattern

θ_{3dB}	3dB Beamwidth
A_m	Maximum attenuation in dB
η	Spectral efficiency in bps per Hz
α	Attenuation factor
γ	Average SINR in dB
i	Sector index
j	Index of the first dominant interfering sector
k	Index of the second dominant interfering sector
u	UE index
b	RB index
M	Number of UEs per sector
N	Number of available RBs per sector
P_b	Power per RB
P_{TN}	Average thermal noise power
$H^{(u,b)}$	Channel gain seen by user u on RB b
$\gamma^{(u,b)}$	SINR over
$I_{i,f}^{(u)}$	Mean interference power averaged over a short-term duration
$G_i^{(u)}$	Interferer group for UE u

π	The set of transmission possibilities of the dominant interferers
$d^{(u)}$	UE demand factor
$I^{(u)}$	Indicator to show whether RB b is restricted or not
$R^{(u)}$	Time average throughput achieved by UE u
$\overline{R}$	Average throughput across all UEs

Chapter 1

Introduction

This chapter serves as an overall introduction to the research done in this thesis. This research was motivated by the 4th generation (4G) networks and their enabling technologies. An overview of 4G networks and their enabling technologies will be given followed by a brief description of the thesis contribution.

1.1 Road to 4th Generation Networks

In the last few years, we have seen an exponential growth in broadband 'always on' communication. Industry trends display tremendous bandwidth growth in mobile broadband networks with smartphones such as Blackberry and iPhone and tablets such as Playbook and iPad now a commonplace occurrence. Industry trends reflect the growing demand on mobile broadband networks because as the sales of smart phones increase and tablets, user expectations also increases. Mobile data use is expected to increase where it is expected that by year 2015, more than 5.6 billion personal devices will be connected to mobile networks and that video traffic will represent up to 66 percent of all mobile data traffic [2, 3].

The growing demand on wireless data traffic is the main motivation of the industry's and academia's investment in orthogonal frequency division multiplexing

(OFDM) based 4G networks. In addition, service providers are looking for cheaper infrastructure and a highly optimized packet switched system in order to meet the higher data rate and Quality of Service (QoS) expectation [4].

1.2 IMT-Advanced

International Telecommunication Union (ITU) is an international entity which is responsible for finalizing the specifications for International Mobile Telecommunication-Advanced (IMT-Advanced) compliant technologies. Long Term Evolution-Advanced (LTE-A) has officially, as of October 2010, met the ITU-Radiocommunication (ITU-R) requirements for IMT-Advanced [5, 6].

The IMT-Advanced specification standards are quite ambitious; the standards span many elements which include cell, cell edge and peak spectral efficiencies, bandwidth and latency requirements which are described more in details as follows [6]:

1. **Spectral Efficiency**

   Spectral efficiency is defined as the aggregate throughput of all users divided by channel bandwidth; it is measurd in bits per second (bps) per Hz. Spectral efficiency requirements are:

   (a) Downlink cell spectral efficiency: from 1.1 to 3 bps

   (b) Uplink cell spectral efficiency: from 0.7 to 2.25 bps per Hz.

   (c) Downlink cell-edge spectral efficiency: from 0.04 to 0.1 bps per Hz

   (d) Uplink cell-edge spectral efficiency: from 0.015 to 0.07 bps per Hz

2. **Bandwidth**

   IMT-Advanced technologies shall be able to support a scalable bandwidth up

	Bits/s/Hz	Speed(km/hr)
Indoor	1	10
Microcellular	0.75	30
Base coverage urban	0.55	120
High speed	0.25	350

Table 1.1: Traffic channel link data rates

to an including 40 MHz.

3. **Mobility**

   There are several mobility classes specified by IMT-Advanced and they are:

   (a) Stationary: 0 km per hour

   (b) Pedestrian: 0-10 km per hour

   (c) Vehicular: 10 to 120 km per hour

   (d) High speed vehicular: 120 to 350 km per hour

   Table 1.1 shows the traffic channel link data rates for different mobility scenarios.

Other specification requirements include control and user plane latency, handover and Voice over IP (VoIP) capabilities which are beyond the scope of this thesis.

1.3 IMT-Advanced Enabling Technologies

To meet the various requirements set by IMT-Advanced, the industry and research academia are investing in techniques that would help achieve those objectives; these techniques are called IMT-Advanced enabling technologies. They include:

1. Wider Band Transmission
2. Multi-Antenna Technologies
3. Coordinated Multi-point Transmission (CoMP)

4. Relaying

1.3.1 Wider band transmission

One of the requirements of IMT-Advanced is to support bandwidth up to and including 40 MHz so as to provision high data rates. At the same time, any 4G system needs to be backward compatible with its predecessor, which supports less bandwidth. Carrier aggregation is used where multiple carriers are accumulated to provide the required bandwidth. This would allow the 4G network to be backward compatible. So for example, LTE-A can exploit the aggregated bandwidth while LTE (its predecessor) would not be able to [7].

Carrier aggregation can be classified into [5]:

1. **Intra-Band Adjacent Carrier Aggregation**: Chunks of adjacent bandwidth carriers from the same band are allocated.

2. **Intra-Band Non-Adjacent Carrier Aggregation**: Chunks of non-adjacent bandwidth carriers from the same band are allocated.

3. **Inter-Band Carrier Aggregation**: Chunks of non-adjacent bandwidth carriers from *different* bands are allocated.

1.3.2 Multi-Antenna Technologies

The use of Multiple Input Multiple Output (MIMO) technology is an integral component for any IMT-Advanced compliant system. In the downlink, it is expected

to support 8X8 antenna configuration, allowing for up to 8 layers to be transmitted simultaneously. This means a possible spectral efficiency exceeding 30 bps per Hz and implying 1G bps data rates in a 40 MHz bandwidth and even higher data rates for bigger bandwidths [7]. Furthermore, spatial multiplexing is included for the uplink; this will allow for up to four layers to be used for the uplink with a potential spectral efficiency of 15 bps per Hz or more [7].

1.3.3 Coordinated Multi-point Transmission

Coordinated multi-point transmission and reception (CoMP) involves coordinating transmission and reception from eNodeBs and user terminals [7]. CoMP is considered for LTE-A as a way to improve the coverage of high data rates and improve both the cell and cell-edge throughput [8].

1.3.4 Relaying

The high data rate expectation necessitates a denser infrastructure which could be implemented using CoMP or by the use of relays [7,9]. Relays are low power transmitter nodes used to reduce the transmitter to receiver distance. With the smaller transmitter to receiver distance, there's a lower pathloss, hence improved cell-edge condition and therefore high data rates. Relays are considered for LTE-A because of its potential to provide high data rates and to improve cell edge throughput. Its also seen as a tool to enhance group mobility and to provide temporary network deployment, as well as improve coverage in new areas [8].

1.4 Thesis Contribution

. LTE-A, an IMT-Advanced compliant technology, will support higher peak rates, higher throughput and coverage, and will have lower latencies thus an improved user experience [10]. To meet the expected growing demand for wireless data services, frequency reuse of 1 is expected to be deployed where all the base stations transmit in the same frequency band. The power constraints on the uplink link budget will necessitate the need for smaller cell sizes compared with the existing networks. The aggressive frequency reuse coupled with the smaller cell sizes will cause interference levels in the network to be quite high, i.e., an interference limited system [11]. An interference limited system will degrade the performance of the network even with the use of IMT-Advanced enabling technologies as described above.

With the high levels of interference produced by the aggressive frequency reuse, there is a need to manage the overall interference in the system to be able to provision higher data applications at higher throughputs and spectral efficiencies. Interference mitigation techniques are used to manage interference levels so that 4G networks can achieve their potential capacity. They play an important role in countering the effect of the generated interference.

One of the interference mitigation techniques that has seen a lot of interest in academia is inter-cell interference coordination (ICIC). ICIC is used to coordinate transmission between multiple base stations so as to minimize the inter-cell interference. In this thesis, we study interference mitigation techniques available in the

literature and we focus on ICIC. The research proposed here is based on the existing work in [12], a dynamic ICIC scheme used to improve cell-edge performance and overall throughput.

The promising ICIC scheme in [12] provides performance gains to cell-edge users and to the overall cell throughput. We implemented this scheme in a network with highly sectored cells. In addition, we enhanced our coordination scheme by including intra-cell coordination on top of the existing inter-cell coordination.

The research submitted here is done in cooperation with Mr. Mahmudur Rahman, the first author in [12] who is a senior PhD student under Prof.Yanikomeroglu. The simulation framework and the scheduling algorithm used in this thesis are taken from Mr. Rahman, modified, and subsequently enhanced as described throughout the thesis. Although the basic algorithm used in this thesis is the same as the one presented in [12], various modifications have been made to implement it in the novel highly sectored cellular network setting.

The work presented in [12] is an inter-cell interference coordination for a multi-cellular network where coordination is between neighboring base stations. The cells considered in [12] have three sectors per base station and inter-cell coordination is considered only. In this thesis, we expand on the previous work by the use of multi-sectored base station where we have twelve sectors per cell site. In addition to the inter-cell coordination considered in [12], we further expand the algorithm by proposing an intra-cell coordination scheme.

The highly sectored base stations used in this thesis combined with the frequency reuse of 1 is expected to increase the cell throughput gain if the interference levels are managed. The twelve sectors per base station generates an unprecedented amount

of inter-cell and intra-cell interference in the network which if left unmanaged would severely compromise the cell-edge throughput. With the proposed schemes we can see that there's a substantial improvement to both network and cell-edge performance with the use of the coordinated transmission compared to no coordination.

1.5 Organization of the Thesis

The organization of this thesis is as follows. Chapter 2 of this thesis provides brief overview of the problem followed by a comprehensive literature review on the inter-cell interference coordination techniques available. Chapter 3 presents the system level simulation parameters. Chapter 4 outlines the proposed algorithm and the problem formulation and Chapter 5 presents the simulation results. In the final Chapter, conclusion of the proposed work is presented and possible future work topics are discussed.

Chapter 2

Literature Review

This chapter outlines the interference problem in 4G networks followed by a general overview of interference mitigation techniques. A detailed description of interference coordination schemes available in the literature is given followed by a preview of the proposed work.

2.1 Interference in 4G Systems

There is a growing demand on mobile data networks to support high rate data applications such as video. This rise in demand for higher rate data applications has lead to orthogonal frequency division multiplexing (OFDM) to be chosen as the key technology for 4G networks [11]. OFDM provides a flexible mean of allocating radio resources as each subcarrier can be allocated, modulated, and coded adaptively; this flexibility allows the network to exploit frequency and multi-user diversity gains. OFDM is also inherently capable of combating inter-symbol interference (ISI) [1]. These advantages makes OFDM an ideal choice for 4G networks where service providers are challenged to increase the capacity and coverage of wireless networks.

In order to increase the network capacity, a frequency reuse of 1 or as close

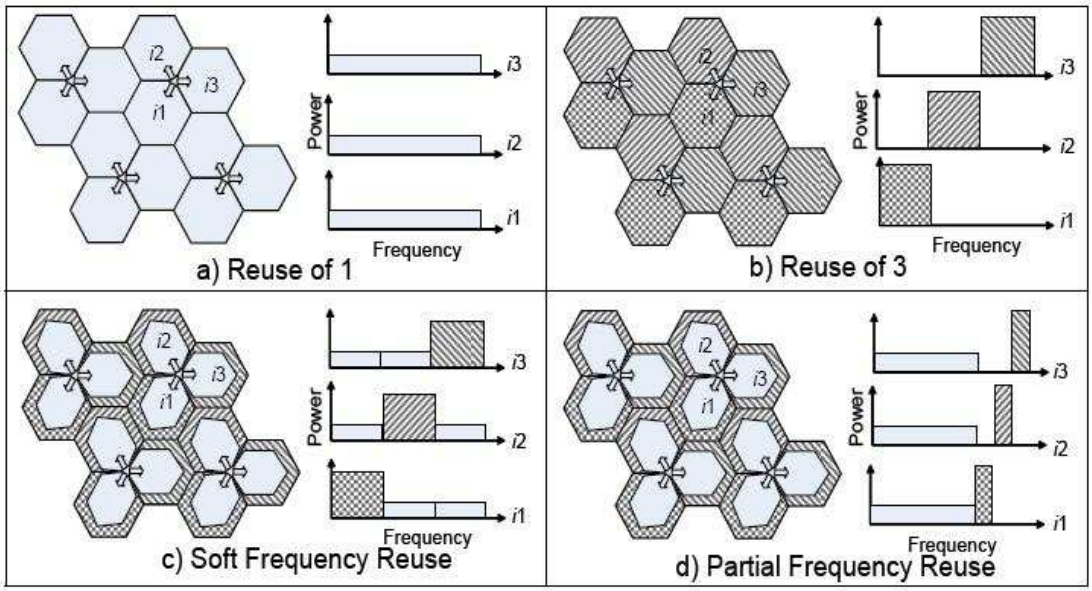

Figure 2.1: Various frequency reuse schemes [1].

to 1 as possible will be deployed in 4G networks [11]. A frequency reuse of 1 means that all sectors will be transmitting in the same frequency band. So for a single eNodeB (or base station) with 3 sectors, all three sectors will be transmitting using the same frequency band. A reuse of 3 on the other hand, means that each sector would be transmitting in a frequency band that is orthogonal to the other sectors so that inter-cell interference is minimized. Figure 2.1 parts a) and b) shows the reuse of 1 and reuse of 3, respectively [1].

In addition to the reuse of 1 in 4G networks, cell sizes are expected to be smaller as is evident by the expected use of heterogeneous networks in LTE-A [10]. This aggressive frequency reuse, coupled with the smaller cell sizes, will generate a substantial amount of inter-cell interference in the network which, if left unresolved, will consequently hinder the performance of the system. Inter-cell interference can be

defined as a collision of resource blocks (RB) where a RB is the smallest granularity time frequency unit used for scheduling [13]. In other words inter-cell interference is caused by RBs colliding due to simultaneous use by several cells. In this context, ICIC techniques aim to minimize collision probabilities and to minimize signal to interference noise ratio (SINR) degradation caused by those collisions [14].

Interference mitigation techniques, in a way, manage interference levels by creating a radio interface that is robust to interference. This would enable mobile networks to increase the capacity of the system without degrading the user's quality of service. Hence, an efficiently utilized spectrum is attainable [15].

In the following sections an overview of interference mitigation techniques available in the literature will be presented.

2.2 Interference Mitigation Techniques: the Solution

There are several methods to mitigate interference that are classified into [1, 15, 16]:

1. Interference randomization aims at randomizing the interference signal by frequency hopping.

2. Interference cancellation aims at demodulating and cancelling interferences through receiver processing.

3. Interference avoidance aims at coordinating and avoiding interference through

resource restriction, also known as inter-cell interference coordination (ICIC).

The focal point of this research is ICIC techniques, which is regarded as a form of CoMP (coordinated multi-point transmission and reception). A simple definition of ICIC can be given as: coordinating transmissions and reception from multiple eNodeBs (or base stations) to manage overall cell interference. In the last few years, ICIC has generated a lot of interest in the industry and academia and it will be adopted in LTE-A. Coordinated transmission is regarded as a tool to improve the capacity and coverage to cell an cell-edge users; it is also expected to increase system throughput in both high loads and low load scenarios [8].

In the next section, an overview of ICIC techniques will be studied. The second half of this chapter focuses on the use of coordinating multiple beams for transmission.

2.3 ICIC in the Literature

2.3.1 Static ICIC

Conventional methods that deal with inter-cell interference include the clustering technique which was used in the 2nd generation (2G) networks. The clustering technique involves partition based transmission, for example, reuse of 3 as shown in Figure 2.1, part b). While the clustering technique is effective in dealing with inter-cell interference, there's a significant resource loss, i.e., all of the available spectrum is not utilized. This resource loss makes the clustering technique impossible to be

adopted by 4G networks where provisioning of high data rates is expected.

An extension of the clustering technique is the fractional frequency reuse (FFR) technique. The use of FFR is motivated by the fact that UE's in the center of a cell are more robust to interference compared to cell-edge users. Cell-edge users, due to their location at the borders of the cell, they experience higher pathloss and they are more prone to interference from neighboring base stations as well. Thus UE's in the center of the cell can tolerate higher reuse compared to cell-edge, hence FFR.

FFR can be classified into:

1. Soft Frequency Reuse (SFR)

   SFR deploys different reuse factors according to the region of the cell whether central or cell edge. A cell is partioned into zones and frequency and power restrictions are done based on the zones. Each zone is allocated transmit power according to the reuse factor while total transmit power is fixed. The cell-edge zone (termed major band) is assigned a higher transmit power compared to the central zone. For example, for a 3 sectored site as shown in Figure 2.1 part c), the cell edge band is assigned one third of the available spectrum which is orthogonal to the bands assigned to neighboring sectors. The central bands (termed the minor band) consists of the frequencies used in the outer zone of the neighboring sectors. The sub-bands are assigned transmission power based on the designated effective reuse factor, with the total transmit power constant. The cell-edge bands are assigned higher transmission power. SFR gives a reuse of 1 and 3, depending on the power assigned [1].

2. Partial Frequency Reuse (PFR)

   Partial frequency reuse (PFR), like SFR, also employs partition based coordination though the implementation varies. PFR restrict the use of resources so that some frequency bands are not utilized in some sectors at all. Figure 2.1, part d) displays the concept of PFR.

3. Adaptive Fractional Frequency Reuse (AFFR)

   Adaptive fractional frequency reuse is basically a dynamic FFR, where the FFR assignments are modified according on the interference levels and channel quality indicators (CQI) taken from UEs [11]

Table 2.1 [11] provides the overall and cell-edge sector throughput for different FFR schemes and for different reuse factors. $N_{reuse} = 1$ and $N_{reuse} = \frac{1}{3}$ is the reuse factor for a reuse 1 and 3, respectively. As seen in the table reuse of 1 provides the best sector throughput but has the worst cell edge throughput. The reuse of 3 cell-edge performance is better than the reuse 1 scheme though with a significant sector throughput degradation. The FFR schemes lie somewhere in between the reuse 1 and reuse 3, which is expected as the reuse is greater than 1 yet still under 3.

	$N_{reuse} = 1$	FFR	$N_{reuse} = \frac{1}{3}$	AFFR
Sector Througphut (Mb/s)	8.01	7.92	6.11	7.89
5th percentile cell-edge througput (kb/s)	286	313	292	312

Table 2.1: Comparison of $N_{reuse} = 1$,$N_{reuse} = \frac{1}{3}$, and AFFR throughputs in a 10 MHz LTE system.

2.3.2 Dynamic ICIC

While static coordination schemes are effective in dealing with inter-cell interference, there's a loss of bandwidth due to partitioning. Such resource loss has been acceptable in early networks, for example Global System for Mobile (GSM), where the focus was only for voice applications. For 4G networks however, where high data application such as video and VoIP are expected to be used, the resource loss will lead to a degradation of overall cell throughput which is undesirable.

In addition, static ICIC require cellular frequency planning which can not be applied to femtocellular networks as femtocells will be placed in an ad hoc manner in the network, thus prior frequency planning will be very difficult [1]. On the other hand, dynamic ICIC requires no prior frequency planning; it relies on channel state information (CSI) gathered from surrounding transmitters.

Dynamic ICIC has attracted in the last few years the attention of academia, industry and different standardization bodies as it is regarded as an essential tool to meet the performance gains promised by 4G networks. There are quite a number of research papers and literature on the topic, some of which we aim to cover in this chapter.

In [17], a decentralized ICIC scheme is considered where the objective is to maximize cell-edge throughput. There is no central controller and coordination takes place between base stations where the base stations allocates subchannels (schedul-

ing unit) in order to maximize cell edge throughput.

In [18], a fractional frequency reuse architecture is proposed where the carriers are partioned into two groups, cell and cell-edge, and the subcarriers are used in both groups to improve the utilization efficiency. An ICIC shceme based on adaptive sub-band avoidance in downlink is used. The schemes improves the channel conditions for cell-edge users, thus improves the overall system throughput.

In [19], an adaptive and distributive interference algorithm is put forward which does not require any prior frequency planning. A multi-cell optimization problem is decomposed into distributed optimization problems by splitting users into two groups: central and cell-edge users. Fairness is considered in this scheme where users are guaranteed a minimum target rate.

A downlink ICIC method for LTE-A is considered in [20] based on the region, where the cell borders are divided into several marked segments. The adjacent cells, with knowledge of the marked segments, will adjust transmission if the interference exceeds a predefined threshold. An example of transmission adjustments is reducing transmission power.

In [1, 21], a downlink multi-cellular ICIC technique is proposed aimed at enhancing cell-edge performance. It's a two function scheme, with the first function is aimed at gathering the dominant interferers and using Hungarian algorithm to the find the restriction requests. The second function lies at the central controller which

resolves any conflicting requests.

In [22], a semi-distributed dynamic scheme is proposed, with the objective of maximizing the overall sector throughput. A dynamic cluster group of interferers is formed together with the transmitting UE where they coordinate among themselves to optimum reuse of resources. The coordination is done between one base station and another; the scheme determines whether a particular chunk (the scheduling unit) should be restricted to use by a certain BS or if it can be used concurrently between different BSs.

In [23], a distributed algorithm is proposed with full frequency reuse with the objective of maximizing the net utility of each cell. An interference price based power allocation algorithm is used to compute the optimum power allocation scheme. The interference pricing is used to coordinate the inter-cell interference between base stations by optimizing resource allocation in each cell. The algorithm does not consider fairness to cell edge users.

A semi-static interference coordination scheme is proposed in [24] based on soft frequency reuse to balance efficiency and fairness. It's a low complexity scheme and the signaling overhead is quite minimal. A best effort utility function is considered, which aims to maximize rate, yet limits the amount of resources that can be allocated to a user with good channel conditions.

Graph based interference coordination schemes have been proposed in [25, 26].

An interference graph is a graphical representation of interference between mobile terminals. It is constructed by evaluating the interference generated to surrounding users when transmitting to a single mobile users.

In [27], a downlink cooperative scheduling of beam transmission framework is proposed taking into consideration spectral efficiencies and user fairness. A fixed number of multiple narrow beams are used to serve mobiles in the downlink. Coordination takes place between sectors that directly face each other.

2.4 Proposed Work

Reference [12], is an extension of the work done in [22]. The focus in [22] was to maximize the overall throughput, whereas [12] includes a fairness factor as the objective is to achieve enhanced cell-edge performance. Another enhancement is the denser reuse of the network which is more in line with IMT-Advanced requirements.

All the previous schemes consider a single antenna per 120 degree sector at the transmitter. To meet the IMT-Advanced requirements, the use of multiple antennas at the base station has become a necessity. Multi-antenna schemes such as spatial multiplexing and beamforming are supported by LTE and LTE-Advance [7, 28]. Up to four transmit antennas (at the base station) and four receive antennas (at the user terminal) will be used in LTE (Rel-8) to provide simultaneous transmission of multiple parallel data streams over a single radio link [7]. A further enhancement is proposed for LTE-A (Rel-10) where it will support up to eight transmission layers for the downlink and up to four transmission layers for the uplink [28]

In our work, we develop a twelve sectored base station with a frequency reuse of 1. We have extended the 6-sectored base station that is described in [29]. The idea of using a multi-sectored base station is inspired by LTE and LTE-A potential spatial multiplexing transmission schemes. We propose an inter-cell and intra-cell interference coordination that is based on the framework of the algorithm proposed in [12]. The proposed schemes are provided as an extension and investigation of previous inter-cell coordination schemes presented. In addition, it investigates the use of a multi-sectored base station.

The use of multiple sectors has been implemented before by Communication Research Center (CRC) Canada in 2004. CRC developed the Milton System (Microwave-Organized Light Network) which is a wireless broadband ethernet network aimed at delivering low cost internet to last mile users. Milton delivers data up to 32 Mbps for the downlink and 11 Mbps for the uplink which makes it suitable for rate hungry application such as broadband internet access, VoIP, and video [30]. Milton deploys 24 identical sector transceiver at the base station where each sector covers an oblong radiation pattern which is about 15 degrees. There are four frequency bands that are used by each base station; the frequency band is used in sequence across the sectors, thus each frequency is used 6 times in a sector.

We conclude by stating that although the use of ICIC has a lot of advantages, it necessitates additional back haul communication and intra-node processing [14].

Chapter 3

System Level Simulation Model

This Chapter introduces the network and system level simulation model used in the implementation of the network model.

3.1 Network Parameters

3.1.1 Fading and Channel Model

The channel model that is used for performance evaluation is based on the Extended Spatial Channel Model (SCME) [31]. It is based on a tapped-delay line structure and the system behavior is simulated across a sequence of drops. The tap delay model is used to construct the wideband channel impulse response. A tap represents angular dispersion at base station and UE; each tap representing a resolvable path or a cluster of scatterers with a different delay. The number of taps used by SCME is fixed at 6 taps which is used in the system level simulation.

Performance of the system under the proposed algorithm is gathered over a series of drops. A drop is defined as one simulation run over a specified time period [31]. The time period is short enough for the assumption that large scale channel parameters remain constant yet small enough to undergo fast fading. The UE position varies

from drop to drop in a random manner.

The small scale fading that is used in the system level simulation is taken from [32]. It's based on time and frequency selective wireless channel. The continuous-time impulse responses is given by

$$h_c(t,\eta) = \sum_{p=0}^{L-1} \gamma_p(t)\delta(\eta - \eta_p(t)), \tag{3.1}$$

and it's a summation of a discrete number of resolvable paths. $\eta_p(t)$ and $\gamma_p(t)$ are time-varying delay and complex gain corresponding to the pth path and L is the number of propagation paths.

$\gamma_p(t)$ can be expressed as

$$\gamma_p(t) = \sum_{r=0}^{M_p-1} \alpha_{r,p} e^{jv_{r,p}} e^{j2\pi(\xi_{r,p}t)}, \tag{3.2}$$

where M_p is the number of rays contributing to the pth path; $\alpha_{r,p}$ is the amplitude, $V_{r,p}$ is the phase, and $\xi_{r,p}$ is the Doppler frequency for the rth ray in the pth path. The frequency response of the time varying channel from equation 3.1 and equation 3.2 is given by

$$H_c(t,f) = \sum_{i=1}^{M} \alpha_i e^{jv_i} e^{j2\pi(\xi_i t - \eta_i f)}, \tag{3.3}$$

where $M = \sum_{p=0}^{L-1} M_p$ is the total number of complex sinusoidal rays in which each ray is specified by the quadruplet $\{\alpha_i, v_i, \xi_i, \eta_i\}$. The sampled channel frequency response at the kth tone of the nth OFDM block can be expressed as

$$H(n,k) \triangleq H_c(nT_{sym}, k\Delta f) = \sum_{i=0}^{M-1} \alpha_i e^{jv_i} e^{j2\pi({}_i n - \tau_i k)}, \tag{3.4}$$

where T_{sym} is the symbol period of the OFDM system with subcarrier spacing of Δf and $f_i = \xi_i T_{sym}$ which is the normalized Doppler frequency in radians. The normalized frequency shift due to time delay is given by $\tau_i = \eta_i \Delta f$.

Equations 3.1 to equation 3.4 are intended to show how the fast fading samples are constructed and are taken from [32].

In the system level simulation, the small scale fading samples were generated prior to any simulation runs. For a single time instant the fading across the channel for a UE speed of 30 km per hour is displayed in Figure 3.1.

3.1.2 Path Loss Model and Shadowing

The large scale path loss which include penetration loss and shadowing is taken from [8]

$$L_D = 128.1 + 10n \log_{10}(D) + L_p + X_\sigma, \tag{3.5}$$

where L_D is the distance dependent path-loss measured in dB, D is the distance separating transmitter and receiver measured in km, L_p is the penetration loss measured in dB, and X_σ is a Gaussian random variable with standard deviation σ in dB to account for shadowing.

3.1.3 Base Station Antenna Pattern, Gain, and Transmit Power

In this layout, we consider a twelve sectored base station (eNodeB) and the user terminal is assumed to be omnidirectional. In [29], there exists a horizontal antenna pattern for 3 sectors and 6 sectors but none for twelve sectored eNodeB. The antenna

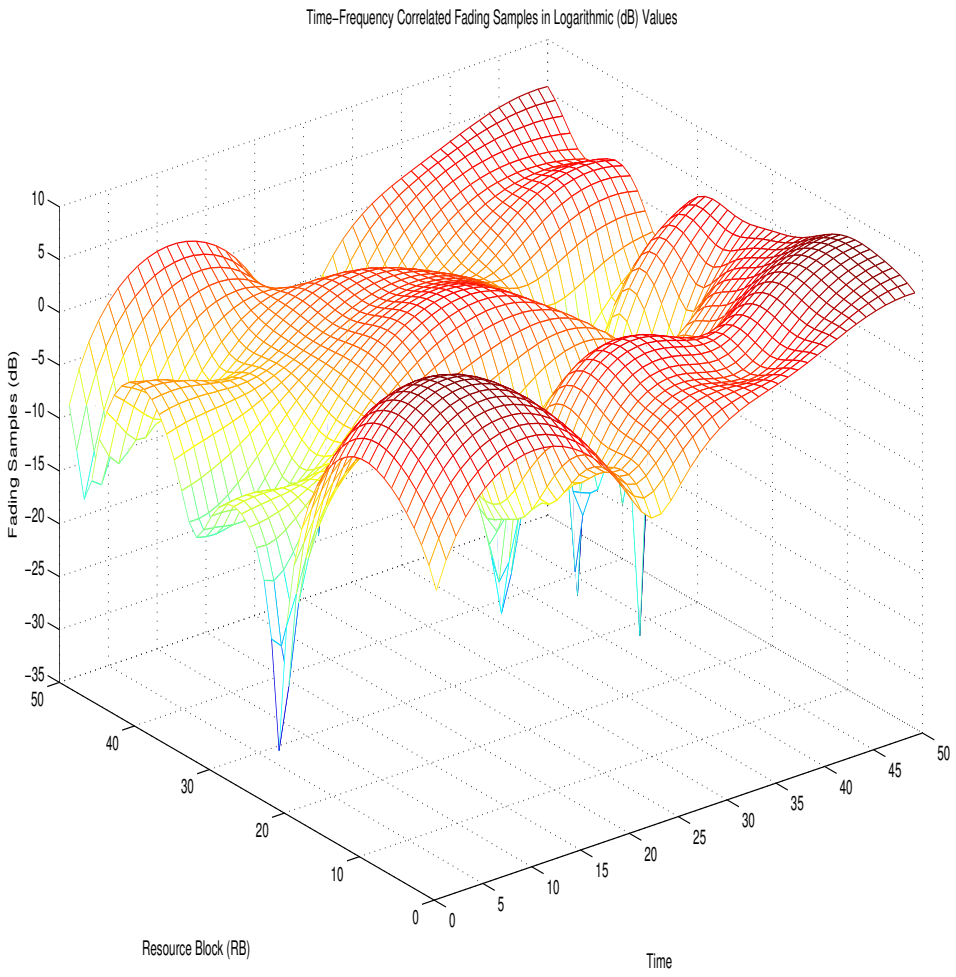

Figure 3.1: Time frequency correlated fading at a single time instant.

pattern is given by

$$A(\theta) = -min\left[12\left(\frac{\theta}{\theta_{3dB}}\right)^2, A_m\right], \tag{3.6}$$

where θ is defined as the angle between the direction of interest and the boresight of the antenna. θ_{3dB} is the 3dB beamwidth and A_m is the maximum attenuation. For a 3 sectored base station, the antenna pattern is given by

$$A(\theta) = -min\left[12\left(\frac{\theta}{\theta_{3dB}}\right)^2, 20\right]. \tag{3.7}$$

In a 3 sectored case, θ_{3dB}=70 degrees and A_m=20 dB and the gain is 14dBi. For 6 sectored base station, the antenna pattern is given by

$$A(\theta) = -min\left[12\left(\frac{\theta}{35}\right)^2, 23\right]. \tag{3.8}$$

The gain for 6 sectors would be 17dBi.

Following the same pattern, 12 sectored antenna pattern is given by:

$$A(\theta) = -min\left[12\left(\frac{\theta}{17.5}\right)^2, 26\right]. \tag{3.9}$$

Accordingly, the gain would be 20dBi.

3.1.4 Lognormal shadowing and Noise Figure

Average thermal noise is computed with a noise figure of 7 dB and indpendent lognormal shadow fading with a standard deviation of 8 dB is considered.

3.1.5 User Equipment Speed and Bandwidth Capabilities

For a UE, it is assumed that the antenna has an omni-directional radiation pattern with antenna gain of 0 dBi [33], and a noise figure of 9 dB. The UE speed is

considered to be 30 km per hour which is used to calculate the Doppler frequency. The UE speed of 30 km per hour is one of the mobility classes (termed vehicular class) defined in [6].

3.1.6 Modulation Scheme

For our modulation scheme, we use a continuous rate adaptive modulation and coding scheme derived from an attenuated and truncated form of Shannon bound that match with link level performance curves for modulation levels of quadrature phase shift keying (QPSK), 16 and 64-quadrature amplitude modulation (QAM) [12, 33]. The code rates range from 1/8 to 4/5.

Relation between SINR and corresponding spectral efficiency is expressed as follows:

$$\eta = \begin{cases} 0; & \gamma < \gamma_{min} \\ \alpha S(\gamma); & \gamma_{min} < \gamma < \gamma_{max} \\ \gamma_{max}; & \gamma > \gamma_{max} \end{cases}, \tag{3.10}$$

where γ is the average SINR seen on a resource block and η is the spectral efficiency in bps per Hz and α is the attenuation factor with respect to the Shannon bound which is:

$$S(\gamma) = \log_2(1 + \gamma). \tag{3.11}$$

Modulation and coding scheme uses α is equal to 0.75 and the maximum spectral efficiency, η_{max}, is 4.8 bps/Hz which is achieved at a maximum SINR of 19.2 dB and the minimum SINR is -6.5 dB below which a RB is unusaable [12, 33].

Chapter 4

Proposed Algorithm

In this chapter, the network layout and the problem formulation of the reference and proposed algorithm are presented. The problem formulation is given for the two schemes presented here: inter-cell interference and intra-cell interference coordination.

4.1 Network Layout

4.1.1 Reference Scheme

The network layout used in this system is derived from baseline simulations test scenarios used in most studies relating to LTE, WIMAX, and WINNER [1, 34]. The reference model consists of 19 cell sites, with an inter-site distance of 500 meters. In the original scheme, each sector has a directional transmit antenna with 120 degree beamwidth. The eNodeB positions and the cellular layout is shown in Figure 4.1. The distribution of antennas, or beams (as it is referenced to here) for our reference scheme, is displayed in Figure 4.2.

4.1.2 Proposed Scheme

Our derived scheme also consists of 19 cell sites, with 12 sectors per sectors per site instead of 3 sectors. In the 3GPP specification [29], the 3 sectored and 6 sectored

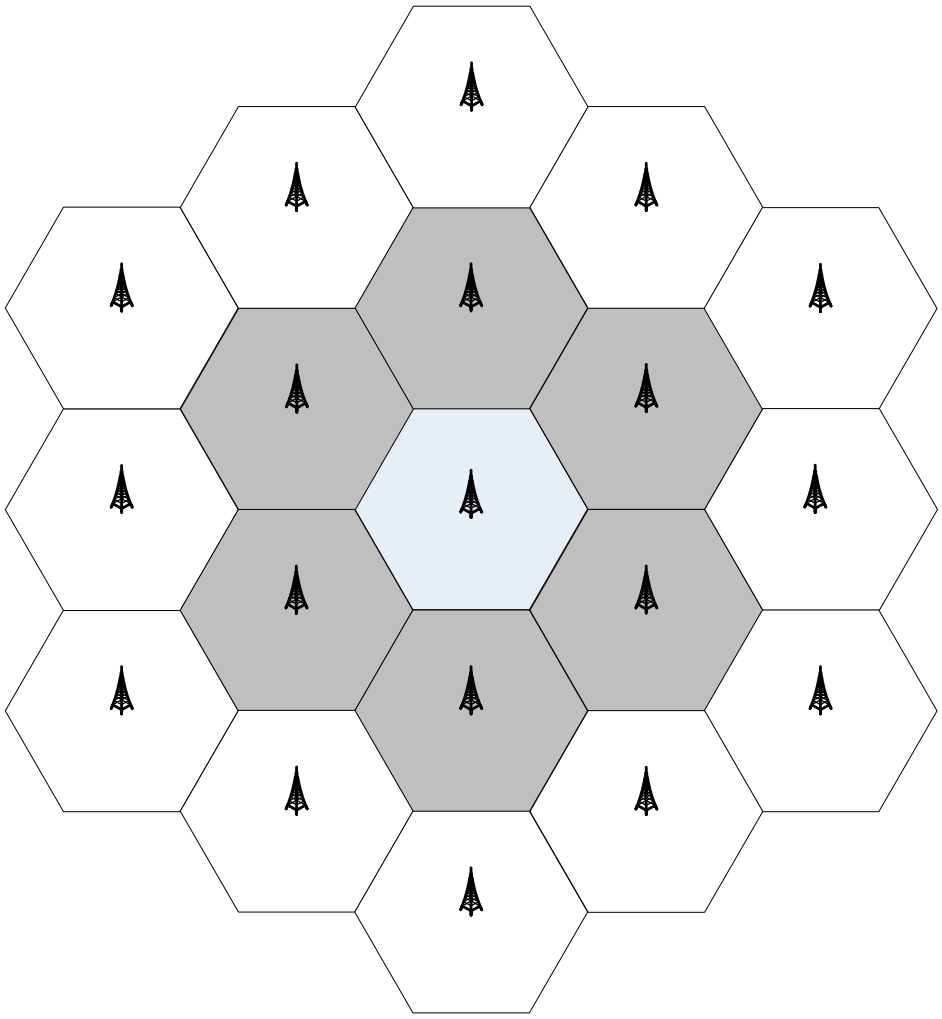

Figure 4.1: Investigated cellular layout.

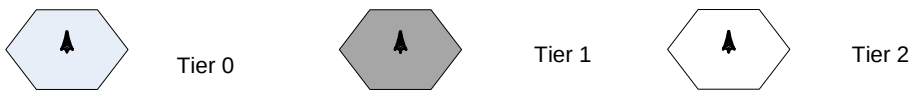

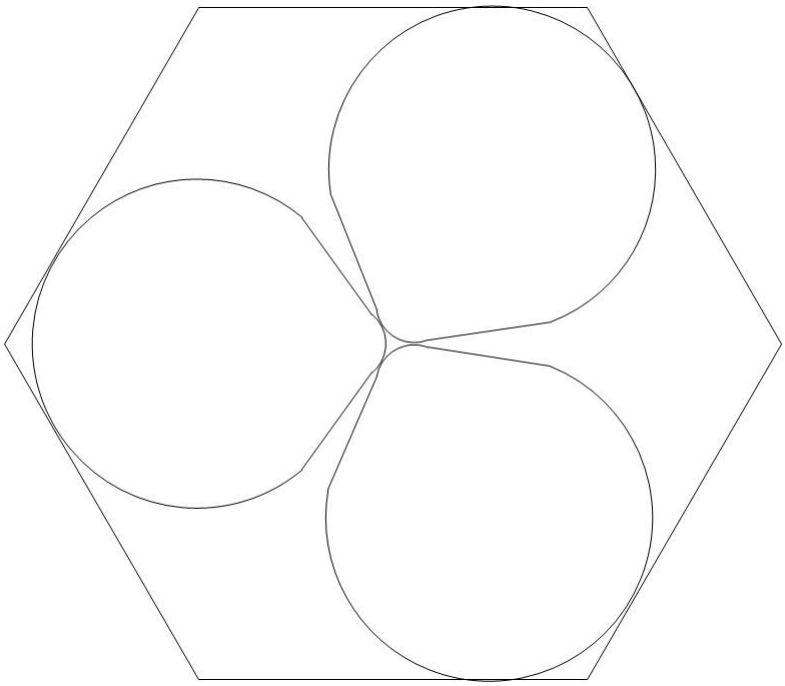

Figure 4.2: Three sectored cell site.

eNodeB were put forward and we derived the 12 sectored site from it. Each sector has a highly directional antenna with 30 degree beamwidth; the corresponding antenna gain pattern for 12 sectored BS is given in Chapter 3. The proposed scheme beam layout is given in Figure 4.3 for the twelve-sectored site.

4.2 UE Placement across a cell site

The user placement model used for the reference and proposed scheme was taken from [35], which places users uniformly in a pie-like sectors so that the resulting combined sectors give a circular shape as shown in Figures 4.4 and 4.5.

Ideally, the sector shape that is used in network level simulation would be a hexagon to avoid the any white spots but this is a close approximation to a hexagon.

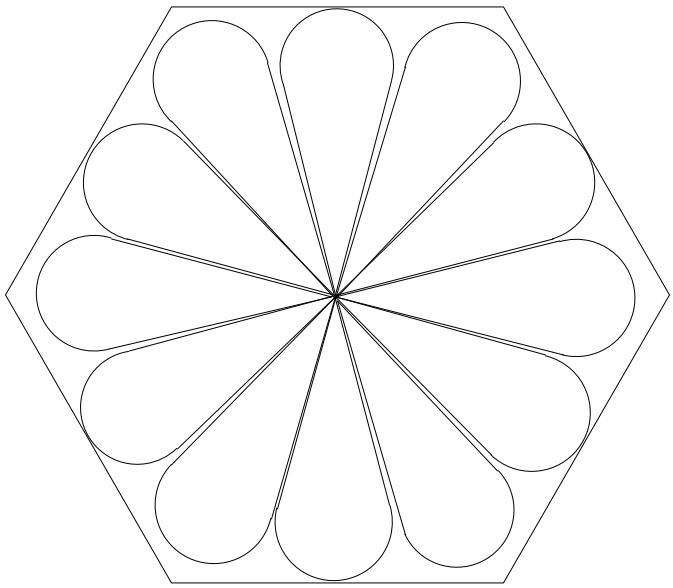

Figure 4.3: Twelve sectored cell site.

A possible solution was to have a bigger circles, i.e., overlapping cell sites but in this case we would not be able to guarantee the same number users per cell per sector. A limitation of the

4.2.1 Reference Scheme

In the reference scheme, users are uniformly distributed across the sectors and base stations where only the seven central base stations (Tier 0 and Tier 1) have users (see Figure 4.3). The outer cell (Tier 2) has no users placed in them as they act as an interference contributer only. In this setup, there are ten users per sector, i.e., a total of 30 users per cell. A MatLab produced diagram shows the UE distribution across the original scheme shown in Figure 4.4.

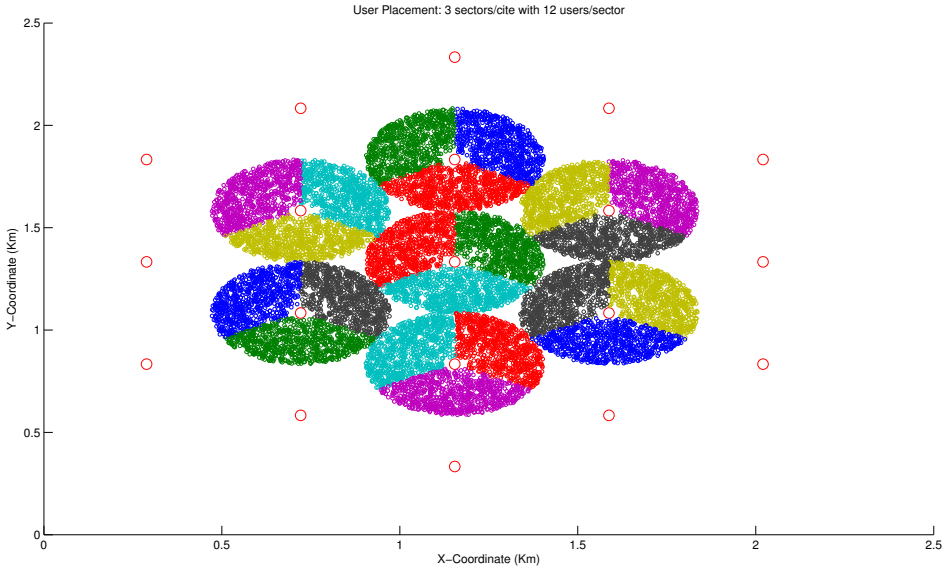

Figure 4.4: UE placement across 3 sectors.

4.2.2 Proposed Scheme

UEs are randomly distributed in the network where in our proposed scheme we have 3 users per sector. UE's are only placed in the seven central cells, where the outer cells do not have any UEs. Figure 4.5 is a MatLab produced diagram that shows the uniform distribution of UEs across twelve-sectored base station across the whole network. The number of users in the sectors for Figure 4.5 and Figure 4.4 is 500 which is done only to clearly show locations and distribution of the sectors and base stations.

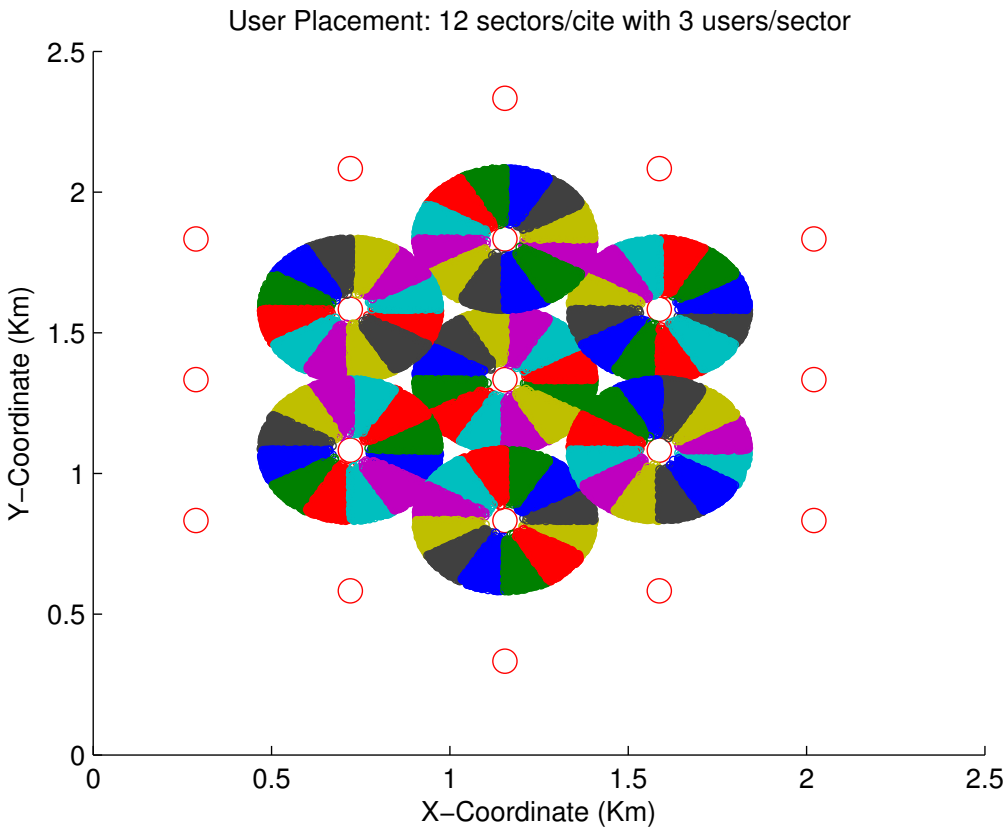

Figure 4.5: UE placement across 12 sectors

4.3 Dynamic ICIC Scheme

The ICIC scheme proposed here is an build upon work that is presented in [12] which is also used as our reference scheme. In the work presented here, eNodeBs coordinate transmission to UEs to minimize the level of interference experienced by UE. In our cellular layout, we have three tiers of cells as seen in Figure 4.1. Tier 0 and Tier 1 have UEs placed in them and take part in coordination; Tier 2 have no UEs and act as an interferer contributor only. The coordinated transmission takes place by restricting, all (two) or partially (one) and possibly none, the most dominant interferers. A detailed description will be given shortly; first a definition of the most dominant interferers will be given.

The most dominant interferers are the two strongest interferers to a transmitting UE and they are based on user location and antenna directivities. They are computed based on large scale fading parameters such as pathloss, transmit antenna gain and shadowing. In our cellular setup, the strongest interferers are usually the neighboring sectors or we call them first tier sectors. Small scale fading parameters are not included for reasons that are specified later in this section.

Take Figure 4.6 for example, users located in Tier 0 are likely to see the strongest interferers from Tier 1. Each numbered sector in figure 4.6 has four sectors but for simplicity's sake, we grouped the four sectors into one 120 degree sector and labeled them as an individual sector. So if we take Tier 0 sectors, the most dominant interferes for each sector would likely be coming from the closest sectors. For sectors 1,

2, and 3, the most dominant interferers would be from:

1. Sector 1: $\{9, 5, 6, 20\}$.

2. Sector 2: $\{9, 10, 12, 13\}$.

3. Sector 3: $\{13, 17, 16, 20\}$.

A downlink transmission scheme based on OFDM will be used in this study and has been also used in [12]. Subcarrier spacing is 15 kHz. Twelve consecutive subcarriers, that span over 7 OFDM symbols, constitutes a resource block (RB) which is the smallest granularity time frequency unit used for scheduling [13]. A 10 MHz bandwidth is used (in a 2.0 GHz band), thus we have a total of 50 RBs per drop used for scheduling.

The reference and proposed scheme are done over a series of steps and can be summarized as follows:

1. A cluster is formed consisting of the transmitter and two most dominant interferers.

2. SINR and corresponding transmission rates are computed based on 4 different transmission possibilities.

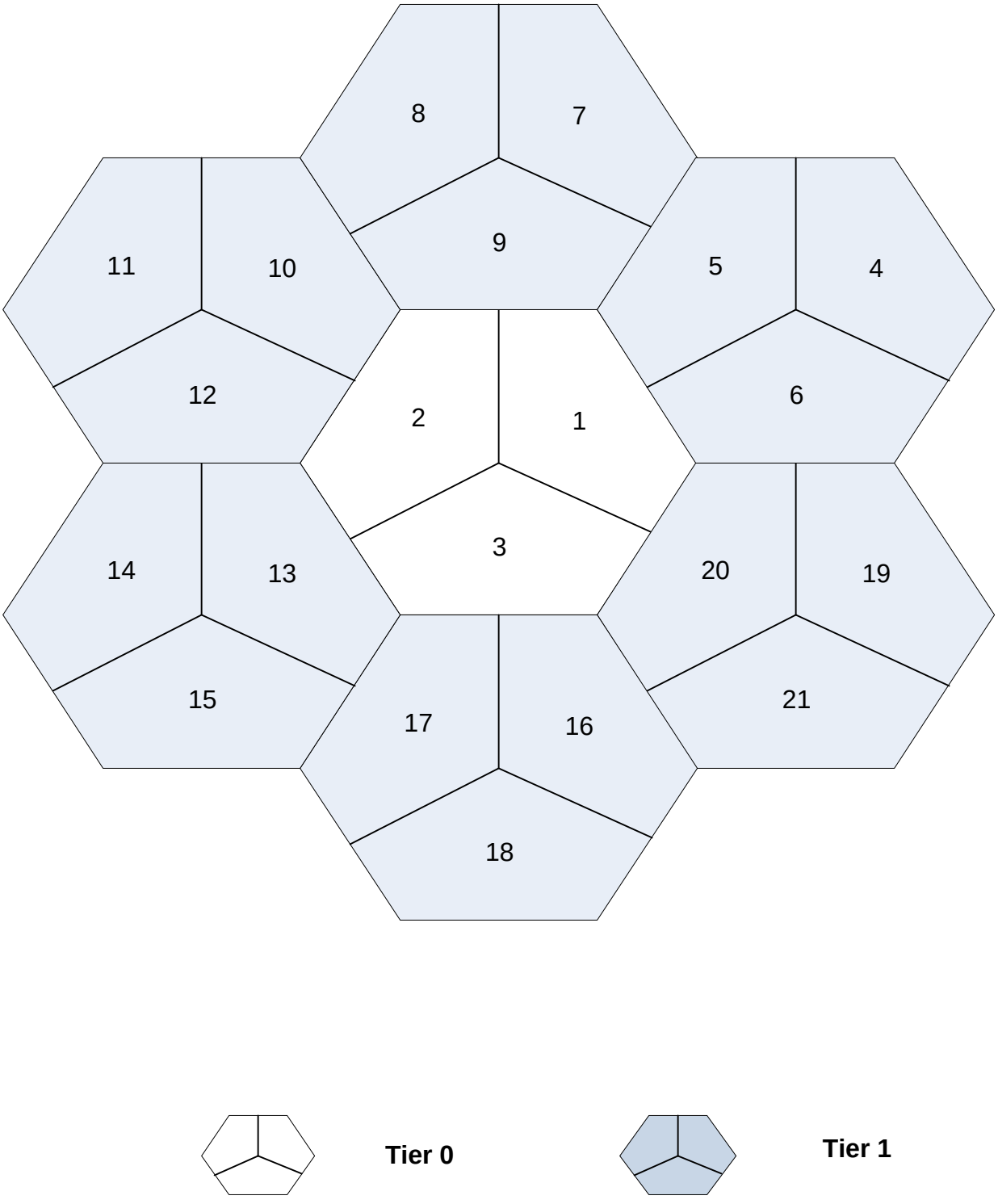

Figure 4.6: Sector layout.

3. An integer linear programming (ILP)method is used to compute the best transmission scheme.

Although the basic steps remain unchanged for the proposed, there are two different implementations of the algorithm which will be explained in detail in the following sections. All the symbols and notations used in this Chapter are based on the notations used in [12].

1. **Cluster Formation**

   Each UE knows the reference of the neighboring first-tier sectors which is based on the following assumption: the system uses cell-specific orthogonal signals and the UE knows the reference signals of the surrounding sectors [12, 13]. The most dominant interfereres are calculated from the first tier sectors as explained earlier. Interference is calculated according to large scale parameters: pathloss, antenna gains and shadowing. For each user, the two maximum interferers are calculated and dynamically grouped for each drop. Using the following expression, mean average interference power over a short duration is computed

   $$I_{i,\mathbf{f}}^{(u)} = P_b.H_{i,\mathbf{f}}^{(u)}, \tag{4.1}$$

   where $\mathbf{f}$ is the set of first-tier dominant interferer sectors, P_b is the transmit power on resource block b, and $H_{\mathbf{f}}$ is the channel gain which includes pathloss, shadowing and antenna gains. $I_{i,\mathbf{f}}^{(u)}$ is sorted according to descending powers of received interference where i is the sector of the transmitting UE u. For each UE, an interferer group is formed with the indices of the highest interfering

sectors, j and k, which is expressed by

$$G_i^{(u)} = \{j, k\}\,. \tag{4.2}$$

The cluster group formed is constant for a *drop* where the user location is unchanged and is based on large scale fading only. Adding short term fading (i.e., multi-path) into account would exponentially increase the complexity of the algorithm which would be computationally prohibitive. This complexity is due to the additional dimension required to take into account the channel variation across a RB.

2. **SINR and Rate Computation**

Using the grouping method described above, we compute the SINR and rates for all UEs. For each user, a cluster group is formed comprised of the transmitting UE and its two most dominant interferers. With this cluster we calculate the possible achievable rates with four possible transmitting scenarios which are defined as follows [12]:

(a) No interferers are restricted, denoted by $r_{i|\{\}}^{(u,b)}$.

(b) Only one interferer j is restricted, denoted by $r_{i|j}^{(u,b)}$.

(c) Only one interferer k is restricted denoted by $r_{i|k}^{(u,b)}$.

(d) The two most dominant interferers j and k are restricted denoted by

$r^{(u,b)}_{i|\{j,k\}}$.

where $r^{(u,b)}_{i|\{\pi\}}$ is the rate for UE u, in sector i on RB b, when π is restricted. The set π is given by

$$\pi = \{\{\}, \{j\}, \{k\}, \{j,k\}\}, \tag{4.3}$$

where π denotes the set of transmission possibilities of the dominant interferer sectors.

SINR is then computed using

$$\gamma_i^{(u,b)} = \frac{P_b H_{i,i}^{(u,b)}}{P_b \sum_{\Psi \neq i} H_{i,\psi}^{(u,b)} + P_b \sum_x H_{i,x}^{(u,b)} . I_x^{(b)} + P_{TN}}, \tag{4.4}$$

where P_b is the transmit power across RB b. $I_x^{(b)}$ is an indicator to show whether RB b is restricted or not with $I_x^{(b)} = 0$ for $x \in \pi$ and $I_x^{(b)} = 1$ for $x \notin \pi$. The channel gains for the desired link is given by $H_{i,i}^{(u,b)}$ and for the interference links it is given by $H_{i,\psi}^{(u,b)}$. P_{TN} denotes the average thermal noise power across a RB.

Using the continuous rate adaptive modulation and coding scheme described in Chapter 3, we compute the rates for the four different transmission schemes.

3. **Use of ILP to Find the Best Transmission Scheme**

The computed rates are then passed to an optimization solver where the interference coordination problem is formulated and solved using an integer linear

programming approach. The problem formulation and the various definitions of the utilities are explained in the subsequent section.

4.4 Problem Formulation: Overview

Conventional scheduling approaches usually aim to maximize overall cell throughput, which puts cell-edge users at a disadvantage. Cell-edge users, due to their location at the outskirts of a cell tend to suffer from a higher path loss in addition to the interference received from neighboring cells. Thus, we consider various utilities to take into account fairness to all the UEs in the network. There are three different utilities considered in the proposed algorithm [12] which take into account a fairness factor and overall cell throughput. The fairness is expressed in terms of the UE demand factor. The UE demand factor is a measure of how rate deprived is a UE and it can be expressed as

$$d_i^{(u)} = \frac{\overline{R}_i}{R_i^{(u)}}, \tag{4.5}$$

where $R_i^{(u)}$ is the average UE u throughput across a certain time frame; which in our algorithm the time frame is 10 past RBs duration. $\overline{R}_i$ is the average throughput of *all* UEs and is given by

$$\overline{R}_i = \frac{\sum_{u=1}^{M} R_i^{(u)}}{M}, \tag{4.6}$$

where M is the total number of UEs per cell. Users with high levels of interference will have low SINR levels, thus will receive poor quality RBs in a conventional scheduling scheme of maximizing the network throughput. The demand factor is the total

throughput of all users in a sector divided by the throughput of a single user in a sector. Thus a UE will have a high demand factor if its radio conditions are poor. When including demand factor in the utility function, cell-edge users are taken into account when scheduling is determined.

The different utilities used in the proposed and reference schemes are [12]:

1. $U_i^{(u,b)} = r_i^{(u,b)}$.

2. $U_i^{(u,b)} = r_i^{(u,b)} d_i^{(u)}$.

3. $U_i^{(u,b)} = r_i^{(u,b)} [d_i^{(u)}]^2$.

The utilities outline above incorporate various degrees of fairness and total cell throughput. The first utility's goal is to maximize rate only whereas the remaining utilities incorporate two levels of fairness: d and d^2. The third utility will be beneficial for cell-edge (rate deprived) users though it will jeopardize to overall throughput.

The different utilities described above are used in the problem formulation where the proposed algorithm is to be solved. The proposed algorithm can be classified into:

1. **Inter-cell interference coordination**: where transmission is coordinated between neighboring cells.

2. **Intra-cell interference coordination**: where transmission is coordinated

between neighboring cells *and* neighboring sectors.

In the following sections a detailed description of the problem formulation for both inter-cell coordination and intra-cell coordination will be given. As the work presented here is an extension of the work in [12], a description of the problem formulation for the reference scheme will also be outlined.

4.5 Problem Formulation: Inter-cell Interference Coordination

Inter-cell interference coordination (IC) involves coordination between neighboring sectors whether sectors covered by a common eNodeB (intra-cell IC) or by neighboring eNodBs (inter-cell IC). In this inter-cell IC scheme, neighbouring eNodeB's determine which RB to be restricted from use to maximize the chosen utility function.

The utility maximization problem is formulated as

$$maximize \sum_{i} \sum_{\pi} [\sum_{u=1}^{M} \sum_{r=1}^{N} U_{i|\Pi}^{(u,b)} \rho_{i|\Pi}^{(u,b)}], \tag{4.7}$$

subject to:

$$\rho_{i|\Pi}^{(u,b)} \in 0, 1; \forall \{u, b\}, \tag{4.8}$$

where ρ is an assignment indicator.

$$I_i^{(b)} = \sum_{\Pi} \sum_{u=1}^{M} \rho_{i|\Pi}^{(u,b)} = \begin{cases} 0; \texttt{RB b is restricted in i} \\ 1; \texttt{otherwise}. \end{cases} \tag{4.9}$$

$I_i^{(b)}$ is a binary integer variable and takes the value of 1 if RB b is assigned to UE u. Equation 4.9 implies that a RB b, if not restricted, can only be used once in a sector.

As described earlier this chapter, there are four transmitting scenarios denoted by $\Pi_i^{(u,b)}$. These scenarios are modeled by the constraints in equations 4.10 to equations 4.13. $I^{(b)}$ is an indicator to show whether RB b is restricted from use by the most dominant interferers.

Inter-cell interferers constraints:

$$\rho_{i|j}^{(u,b)} + I_j^{(b)} = \{0, 1\}, \tag{4.10}$$

$$\rho_{i|k}^{(u,b)} + I_k^{(b)} = \{0, 1\}, \tag{4.11}$$

$$\rho_{i|\{j,k\}}^{(u,b)} + I_j^{(b)} = \{0, 1\}, \tag{4.12}$$

$$\rho_{i|\{j,k\}}^{(u,b)} + I_k^{(b)} = \{0, 1\}. \tag{4.13}$$

Equations 4.10 to equation 4.13 model the inter-cell interference constraints. This is a binary integer linear programming formulation where the assignment values are either 1 or 0. With this current setup, either $\rho_{i|j}^{(u,b)}$ is equal to 1 or $I_j^{(b)}$ is equal to one.

There are 4 different dominant transmission possibilities on a RB b which is denoted by $\Pi_i^{(u,b)}$. For transmitting UE u in sector i, with the first and second dominant interferers of j and k, respectively, then the four transmission possibilities are

1. No restriction on RB b by sectors j and k which is denoted by $I_j^{(b)} = 1$ and $I_k^{(b)} = 1$ with an achievable rate of $r_{i|\{\}}^{(u,b)}$.

2. RB b is restricted from use by sector j only which is denoted by $I_j^{(b)} = 0$ and $I_k^{(b)} = 1$ with an achievable rate of $r_{i|\{j\}}^{(u,b)}$.

3. RB b is restricted from use by sector k only which is denoted by $I_j^{(b)} = 1$ and $I_k^{(b)} = 0$ with an achievable rate of $r_{i|\{k\}}^{(u,b)}$.

4. RB b is restricted from use by sectors j and k which is denoted by $I_j^{(b)} = 0$ and $I_k^{(b)} = 0$ with an achievable rate of $r_{i|\{j,k\}}^{(u,b)}$.

For equation 4.10, for a user u, in sector i, a RB b is either restricted from use by the most dominant interferer (sector j) or not restricted to use. The second equation 4.11 portrays the restriction on the second most dominant interferer and so on.

The two most dominant interferers, sector j and k will also have their own set of restrictions and this inter-relation constraint propagates in the network. The optimizer then decides the optimal overall scheme that is based on the chosen utility and decides which restrictions should be imposed i.e. its a centralized scheme.

There are a large number of variables and constraints that are fed into the optimizer which consequently increases the complexity of integer programming. Therefore we decompose the problem into smaller sub-problems and then the optimizer solves the problem in an iterative manner. Thus, the optimizer takes sets of RBs of size κ (sub-problem size) and an assignment solution is found. In the case of inter-cell

interference coordination, κ is taken to be 10 RBs.

RB assignment to a specific UE constraint:

$$\sum_{\Pi} \sum_{b} \rho_{i|\Pi}^{(u,b)} \leq \beta; \forall \{i, u\}, \tag{4.14}$$

where the value of β is 4.

4.6 Effect of Value of β and κ for Inter-Cell Coordination

In the inter-cell coordination scheme, κ is taken to be equal 10, and since the total number of RBs is 50, the problem is decomposed into 5 smaller subproblems which is fed into the optimizer for an assignment problem. With the constraint expressed in 4.14 a maximum of 4 RBs can be assigned to a UE per subproblem or iteration. This constraint is put in place to avoid excessive resource assignment to a single UE. The value of κ was chosen in such a way to ensure that all UEs would receive a minimum amount or RBs per iteration.

In this setup, we have three users per sector and the value of κ and β are 10 and 4, respectively; this means that the 3 users are guaranteed a minimum of 2RB up to a maximum of 4 RBs per iteration. Limiting the value of β would hinder the total cell throughput as this means that UEs are not receiving enough RBs (i.e. assigned a smaller bandwidth, thus smaller rate capability). Controlling the values of κ and β ensures that the outage remains low and yet at the same time, network throughput is not affected.

4.7 Problem Formulation: Intra-cell Interference Coordination

Intra-cell interference coordination was thought of as a beam selection algorithm, where coordination takes place between sectors under serving base station to determine which beam, which RB is best suitable for use. It minimizes the overall interference in the cell. Intra-cell IC involves coordination between neighboring (eNodeBs) and a further coordination takes place between sectors within the same eNodeB. From Figure 4.7 we can see the beam distribution in a cell site. The additional transmission constraint involves restricting the use of a RB to only once in a a beam group to optimize the chosen utility function. A beam group comprises 4 sectors in a 120 degrees beamwidth. Take Figure 4.7 for example, there are three beam groups:

- Beam Group A: consists of sectors (1-4)

- Beam Group B: consists of sectors (5-8)

- Beam Group C: consists of sectors (9-12)

The optimizer decides which RB restrictions are to be forced. This is implemented on top of the inter-cell IC taking place as described in the previous section.

In this setup, a maximum of 25 percent of all the resources will be utilized. In this context, the level of interferers in the network will be down to a quarter of its initial value. This is why SINR calculation has been modified to

$$\gamma_i^{(u,b)} = \frac{P_b H_{i,i}^{(u,b)}}{P_{b_{Reduced}} \sum_{\Psi \neq i} H_{i,\psi}^{(u,b)} + P_b \sum_x H_{i,x}^{(u,b)} . I_x^{(b)} + P_{TN}}, \tag{4.15}$$

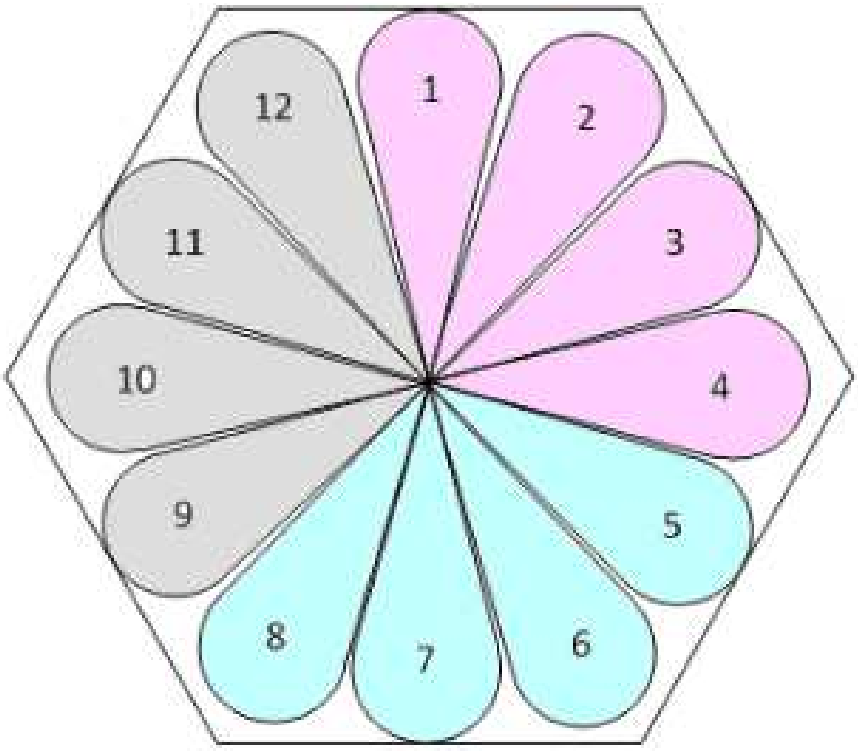

Figure 4.7: Intra-cell Coordination.

where $P_{b_{Reduced}}$ is equal to $0.25 * P_b$.

The utility maximization problem is formulated as

$$maximize \sum_{i} \sum_{\pi} [\sum_{u=1}^{M} \sum_{r=1}^{N} U_{i|\Pi}^{(u,b)} \rho_{i|\Pi}^{(u,b)}], \tag{4.16}$$

subject to:

$$\rho_{i|\Pi}^{(u,b)} \in 0, 1; \forall u, b], \tag{4.17}$$

$$I_i^{(b)} = \sum_{\Pi} \sum_{u=1}^{M} \sum_{\phi} \rho_{i|\Pi}^{(u,b)} = \begin{cases} 0; & \texttt{RB b is restricted in i} \\ 1; & \texttt{otherwise} \end{cases}, \tag{4.18}$$

where ϕ denotes the beam group. Each cell site has three beam groups as described

earlier.

Inter-cell interferers constraints

$$\rho_{i|j}^{(u,b)} + I_j^b = \{0,1\}\,, \tag{4.19}$$

$$\rho_{i|k}^{(u,b)} + I_k^b = \{0,1\}\,, \tag{4.20}$$

$$\rho_{i|\{j,k\}}^{(u,b)} + I_j^b = \{0,1\}\,, \tag{4.21}$$

$$\rho_{i|\{j,k\}}^{(u,b)} + I_k^b = \{0,1\}\,. \tag{4.22}$$

Equations 4.19 to equations 4.22 play the same role as the first part of the algorithm as described in Section 4.5. They model the inter-cell interference constraints.

RB assignment to a specific UE constraint

$$\sum_{\Pi}\sum_{b} \rho_{i|\Pi}^{(u,b)} \geq \beta; \forall\,\{i,u\}\,. \tag{4.23}$$

4.8 Effect of Value of β and κ for Intra-Cell Coordination

The complexity of linear programming algorithm is quite high which is why the problem is decomposed into smaller sub-problems and solved iteratively by the optimizing tool. The number of RBs to be allocated to UEs is equal to 50, so the problem is decomposed into κ RBs to be assigned to UEs which is done in an iterative fashion. The size of κ and β in this scheme are 16 and 2, respectively. The constraint in equation 4.23 was put in place to avoid excessive RB allocation to a single UE.

Due to the difference in the problem formulation, κ here is taken to be equal to 16 compared to the inter-cell coordination scheme. In this scheme, RB assignment is done for a beam group which has 12 users compared to RB assignment done for a single sector with three users, as with the previous scheme. As an example, if we were to use a κ size of 10 and a β size of 4, in a worst case scenario this could mean 75 percent of the UEs not assigned any RBs (with the assignment of 4, 4, and 2 RBs to three UEs).

The values of β and κ were chosen so as to balance the overall throughput versus the cell outage. Which RB to be assigned to a UE and the quality of RBs (i.e. either low or high SINR RBs) is decided by the optimizer according to the utility scenario chosen.

4.9 Problem Formulation: Reference ICIC Scheme

In [12], a dynamic ICIC scheme was used with the system model described in Figure 4.1. In each cell site there are three sectors, in each sector there are 10 UEs that are uniformly placed in each sector. Conventional scheduling methods usually aim to maximize overall cell throughput. These scheduling schemes are unjust to cell-edge users as they are overlooked in the scheduling process due to their poor to the system throughput. Cell-edge users due to their location at the border of the cell, tend to suffer from worst radio conditions compared to users in the cell-center. The unfairness is treated by the author in [12] by including a demand factor as explained in Section 4.4.

As the proposed scheme is based on [12], the original problem formulation will be proposed here.

The utility maximization problem is formulated as

$$maximize \sum_{i} \sum_{\pi} [\sum_{u=1}^{M} \sum_{r=1}^{N} U_{i|\Pi}^{(u,b)} \rho_{i|\Pi}^{(u,b)}], \tag{4.24}$$

subject to:

$$\rho_{i|\Pi}^{(u,b)} \in 0, 1; \forall \{u, b\}, \tag{4.25}$$

where M is the number of UEs in a cell and is equal to 10. Π is the set of transmission possibilities of the dominant interferer sector and N is the number of available RBs per sector. ρ is an assignment indicator and $I_i^{(b)}$ is a binary integer variable and takes the value of 1 if RB b is assigned to UE u.

$$I_i^{(b)} = \sum_{\Pi} \sum_{u=1}^{M} \rho_{i|\Pi}^{(u,b)} = \begin{cases} 0; \texttt{RB b is restricted in i} \\ 1; \texttt{otherwise}. \end{cases} \tag{4.26}$$

Equation 4.26 implies that a RB b, if not restricted, can only be used once in a sector.

Inter-cell interference constraints are used

$$\rho_{i|j}^{(u,b)} + I_j^{(b)} = \{0, 1\}, \tag{4.27}$$

$$\rho_{i|k}^{(u,b)} + I_k^{(b} = \{0, 1\}, \tag{4.28}$$

$$\rho_{i|\{j,k\}}^{(u,b)} + I_j^{(b} = \{0, 1\}, \tag{4.29}$$

$$\rho_{i|\{j,k\}}^{(u,b)} + I_k^{(b} = \{0,1\}\,. \tag{4.30}$$

Equations 4.27 to 4.30 model the different transmission possibilities as denoted by Π.

4.10 Effect of Value of β and κ for ICIC in Reference Scheme

Due to the high complexity of the algorithm, it is split into several subproblems, each subproblem takes a subset κ and finds an assignment solution. For the reference scheme the value of κ is 10 RBs. To avoid excessive resource block allocation to a single block the constraint in 4.31 was put in place.

RB assignment to a specific UE constraint:

$$\sum_{\Pi}\sum_{b}\rho_{i|\Pi}^{(u,b)} \leq \beta; \forall\,\{i,u\}\,, \tag{4.31}$$

where the value of β is 2.

Chapter 5

Simulation Results

This chapter showcases the simulation results of the implemented schemes. Description of the simulation framework, system parameters used is given, as well as the performance indicators used for analysis. Finally, the simulation results are presented.

5.1 System Layout

A total of 19 cells have been used in the system level simulations. UE's are only dropped in Tier 0 and Tier 1 (see Figure 5.1). Tier 2 is also considered in the system layout but there are no UEs and it acts as an interferer contributer only. It's assumed that all the subchannels in Tier 2 are used, i.e., 100 percent loading.

The system level simulation is executed over a series of drops. A drop is defined as one simulation run over a specified time period, which in this setup a drop is simulated for a 50 RB time duration. Since Tier 2 acts only as an interferer contributer, statistics collected from Tier 1 will not be a realistic reflection of the algorithm; thus the results presented in this section are calculated from Tier 0 only.

5.2 Performance Indicators

There are several performance indicators that is used in this thesis to analyze the statistics collected of our proposed scheme. As mentioned earlier, this work has been

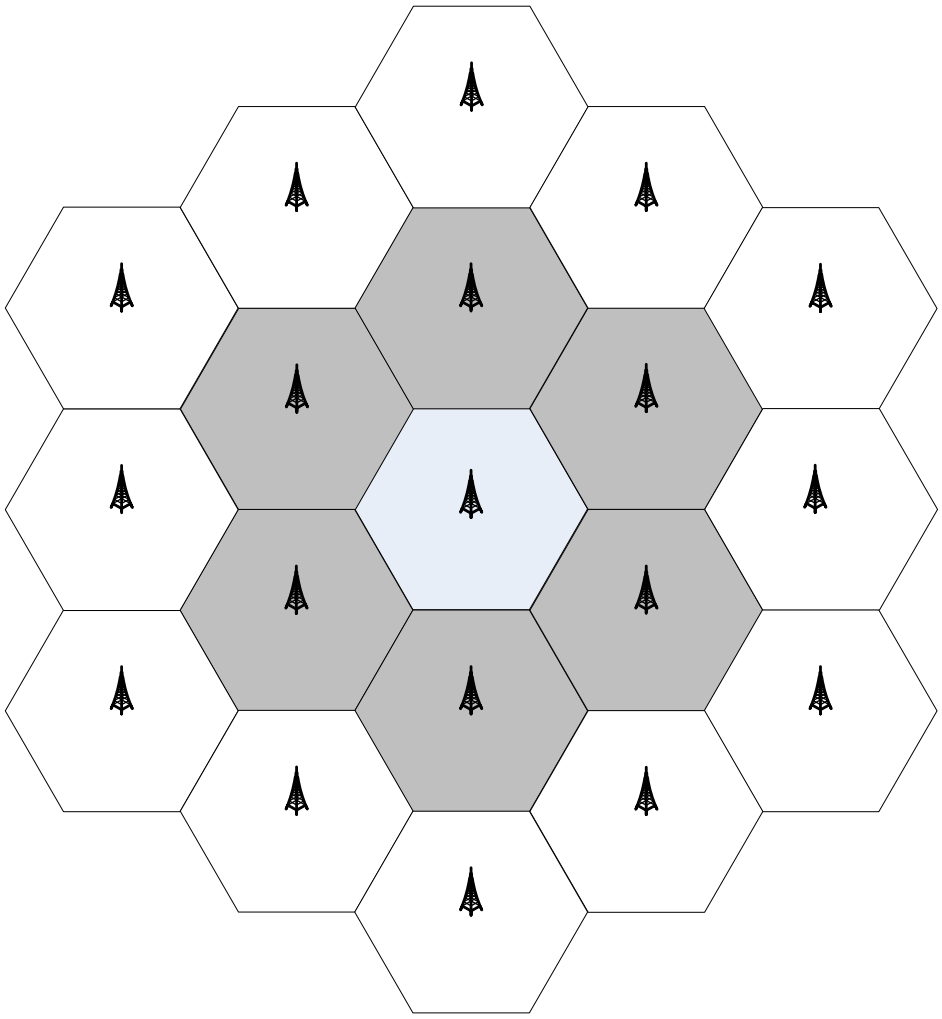

Figure 5.1: Investigated system layout.

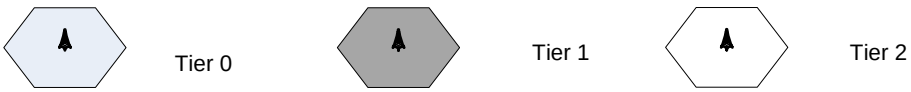

built on an a recently proposed ICIC scheme. To measure the performance gains, the following performance indicators have been used:

- CDF of average UE throughput: we use cumulative distribution function (CDF) of the average UE throughput to measure the performance of the algorithm. The 5th percentile throughputs are taken as measures of the cell-edge throughput.

- Spectral Efficiency (central and cell-edge): Defined as the aggregate throughput of all the users divided by channel bandwidth and it is measured in bits per second per Hz. Cell-edge user spectral efficiency is defined as the 5th percentile point of CDF of user throughput [6].

- RB utilization in each sector: Although ICIC schemes provide performance gains to cell-edge and total cell throughput, they cause RBs to be restricted from use. It is used to measure the percentage of unused spectrum due to ICIC.

We have executed the algorithm for the three different utilities for both inter-cell coordination and the intra-cell coordination. The user demand d_i is computed from the past throughput achieved over the last 10 RBs duration. In the following section, simulation results will be presented for the different utilities explained in Chapter 4. The results are always compared to the reference scheme [12] and its also compared to the scenario where there's no coordination at all.

The reference scheme was originally implemented for 10 users per sector. We have modified the reference scheme and implemented it on 12 users per sector so it would be a fair comparison of the proposed scheme. The reference scheme results that are presented here are executed on 12 users per sector instead of 10.

To simulate our system and proposed algorithm, we have used MATLAB and two optimization solvers YALMIP [36] and TOMLAB [37]. The parameters used for simulation are outline in Table 5.1.

Cellular layout	Hexagonal grid, 19 cell sites, 12 sectors per site
Inter-site distance	500m
Carrier frequency	2.0 GHz
Bandwidth	10 MHz (50 RBs)
Lognormal shadowing	Independent among links
Shadowing standard deviation	8 dB
UE speeds	30 km/hr
Penetration loss	10 dB
Transmit antenna configuration	4 antennas/sector
Receive antenna configuration	Single omni-directional antenna
eNodeB antenna gain	26 dBi
UE antenna gain	0 dBi
UE noise figure	7 dB
AMC modes	Attenuated Shannon bound for QPSK, 16 and 64-QAM with varying rates
Channel model	6-Tap SCME
Total sector TX power	11.5 dBm
UE close-in distance	35 m
Traffic model	Full buffer

Table 5.1: System and Simulation Parameters.

5.2.1 Reference Scheme

The scheme that is used in this thesis as a reference is the scheme proposed in [12], whose algorithm and problem formulation is defined in section 4.9. The original reference scheme was simulated for 10 users per 120 degree sector. In our proposed scheme, we simulated the algorithm for 12 users per 120 degree sectors. To be consistent, the reference scheme results were regenerated for 12 users per sector instead of the original 10.

5.3 Simulation Results: Analysis

5.3.1 Utility $U = rd$

For the utility $U = rd$, we generated CDF plots of the UE throughput for both inter-cell and intra-cell interference coordination which are given by Figures 5.2 and 5.3, respectively. The performance statistics computed is further discussed next.

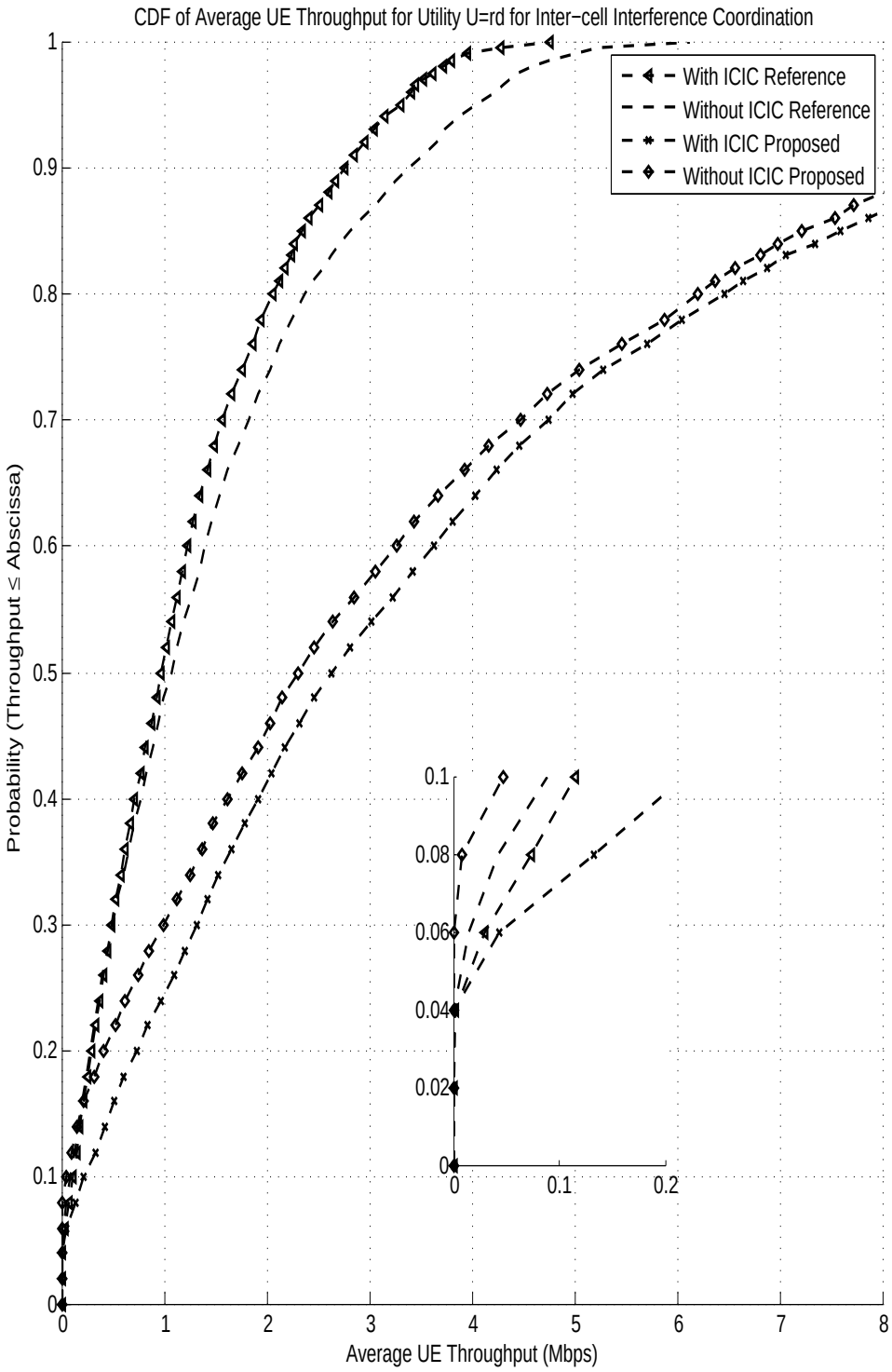

Figure 5.2: CDF of average UE throughput for inter-cell interference coordination $U = rd$.

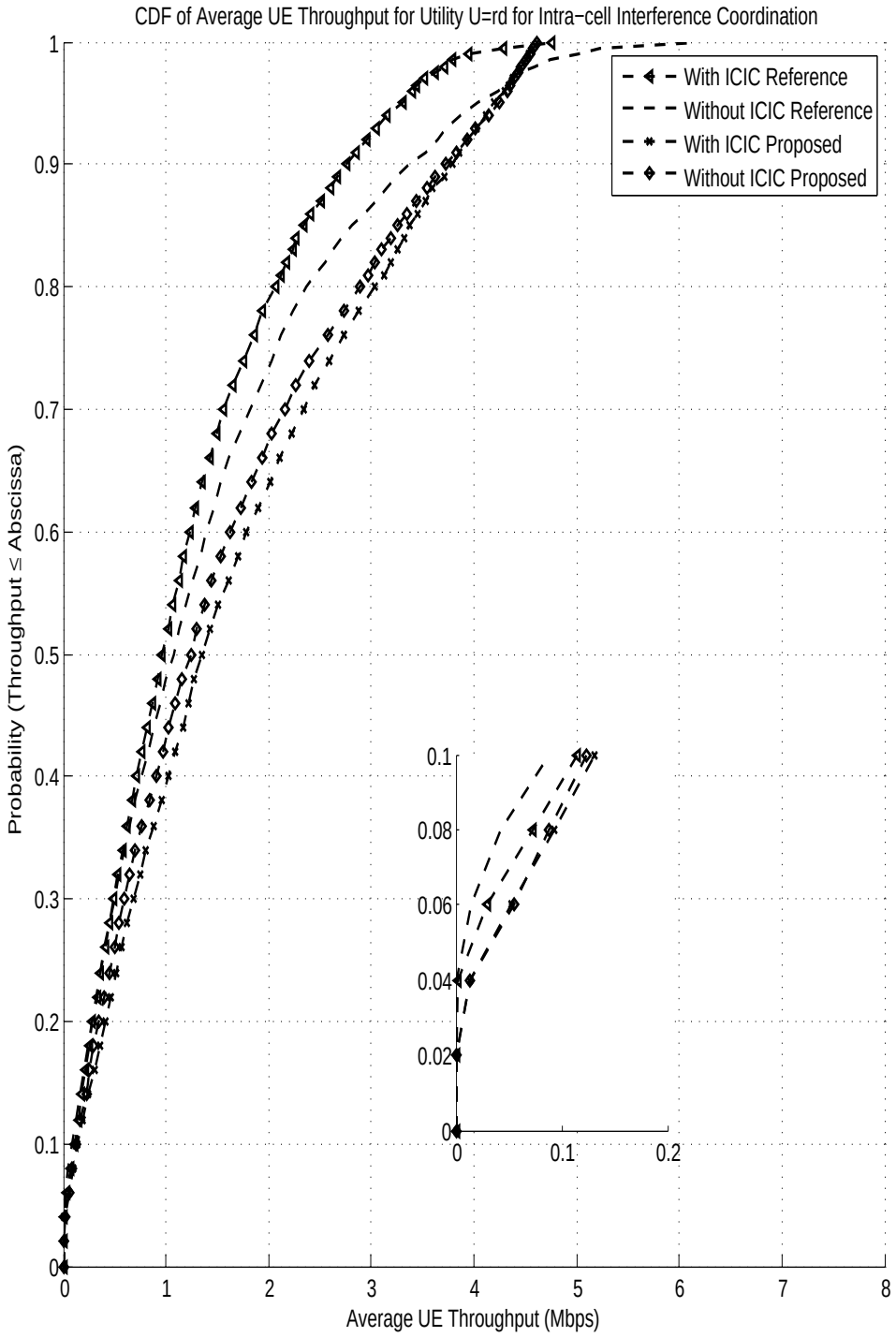

Figure 5.3: CDF of average UE throughput for intra-cell interference coordination $U = rd$.

Performance Indicators:

1. Sector and Cell UE throughput:

   In Table 5.2, sector and cell UE throughput are given. We can observe that inter-cell coordination the cell throughput is almost tripled compared to reference scheme where in intra-cell coordination the cell throughput is 1.5 times the reference scheme. We also see an overall improvement when using an ICIC scheme compared to no ICIC at all.

Version	Sector Throughput (Mbps)	Cell Throughput (Mbps)
Reference Scheme	14.28 (12.89)	42.84 (38.67)
Inter-cell Coordination	11.18 (10.37)	134.16 (124.49)
Intra-cell Coordination	5.03 (4.75)	60.45 (57.20)

Table 5.2: Sector and cell throughput for $U = rd$. Values in brackets correspond to no ICIC at all.

2. Sector cell-edge and total cell-edge throughput

   In Table 5.3, sector cell-edge and total cell-edge spectral efficiency are given. From the results, we can conclude that the cell-edge performance has seen a significant improvement compared to the reference scheme. From the zoomed tail of the CDF of the Figure 5.2 and Figure 5.3, we can observe the 5th percentile point for inter-cell and intra-cell schemes, respectively.

Version	Sector Cell-Edge Throughput (kbps)	Total Cell-edge Throughput (kbps))
Reference Scheme	11.81 (2.67)	35.45 (8.01)
Inter-cell Coordination	12.45 (0)	149.42 (0)
Intra-cell Coordination	35.71 (32.03)	428.63 (384.45)

Table 5.3: Sector cell-edge and total cell-edge throughput for $U = rd$. Values in brackets correspond to no ICIC at all.

3. Cell and Cell-Edge Spectral Efficiency:

   In Table 5.4, sector and cell spectral efficiency are given. We can observe that the spectral efficiency is highest for inter-cell coordination for total cell throughput. Intra-cell coordination provides the highest spectral efficiency for cell-edge users. We can also note that the performance of the proposed schemes exceeds that of the reference scheme for both the three schemes. When comparing intra-cell with inter-cell coordination, we notice that that the reference scheme is much lower compared to proposed. This could be attributed to the lower level of interference in intra-cell coordination scheme.

Version	Cell Spectral Efficiency (bps/Hz)	Cell-Edge Spectral Efficiency (bps/Hz)
Reference Scheme	4.28 (3.86)	0.0035 (0.0008)
Inter-cell Coordination	13.42 (12.45)	0.0149 (0)
Intra-cell Coordination	6.05 (5.72)	0.0428 (0.0384)

Table 5.4: Cell and cell edge spectral efficiency for $U = rd$. Values in brackets correspond to no ICIC at all.

4. Percentage of RB utilization

   RB percentage of utilization across a cell is given in Table 5.5. The reference scheme sees the highest amount of utilization compared to the other schemes. As expected the maximum utilization for intra-cell interference for all utilities was 25 percent. We observe that for the reference schemes that RB utilization always exceeds or equal to that of the ICIC which falls in line with the fact that ICIC restricts RBS from use.

Version	Resource Block Utilization %
Reference Scheme	85.67 (99.47)
Inter-cell Coordination	67.47 (68.24)
Intra-cell Coordination	24.00 (23.98)

Table 5.5: Percentage of RB utilization for $U = rd$. Values in brackets correspond to no ICIC at all.

5.3.2 Utility $U = r$

For the utility $U = r$, the CDF plots of UE throughput for both inter-cell and intra-cell interference coordination which are given by Figures 5.4 and 5.5, respectively. The performance statistics computed is further discussed next.

Performance Indicators:

1. Sector and Cell UE throughput:

   In Table 5.6, sector and cell UE throughput are given. Once again, the cell throughput compared to the reference scheme is almost thrice improved for inter-cell coordination. For intra-cell coordination cell throughput improvement is almost 1.5 times the reference scheme.

Version	Sector Throughput(Mbps)	Cell Throughput(Mbps)
Reference Scheme	15.63 (13.75)	46.89 (41.25)
Inter-cell Coordination	11.84 (10.53)	142.11 (126.35)
Intra-cell Coordination	5.55 (5.13)	66.67 (61.52)

Table 5.6: Sector and cell throughput for $U = r$. Values in brackets correspond to no ICIC at all.

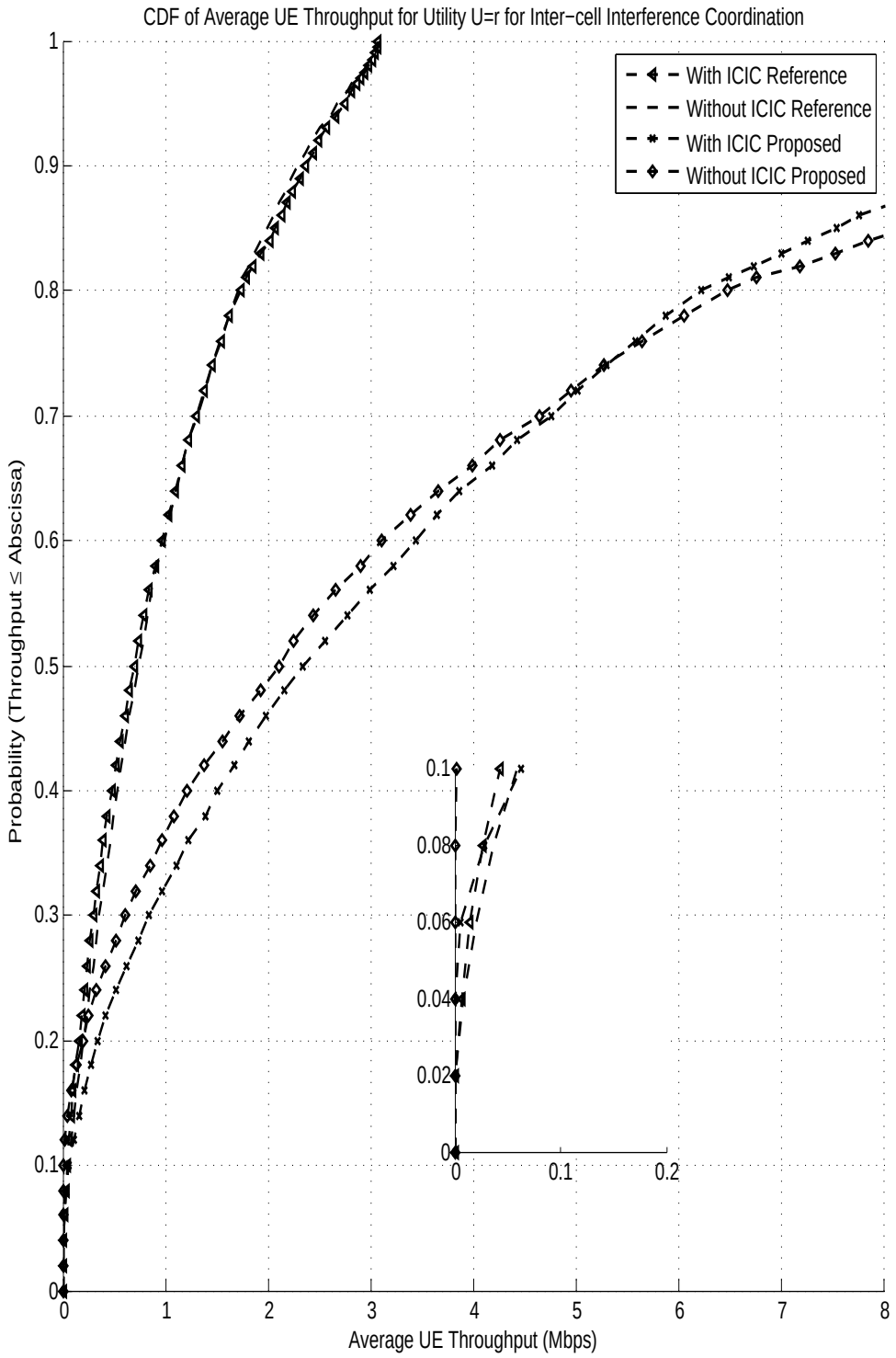

Figure 5.4: CDF of average UE throughput for inter-cell interference coordination for $U = r$

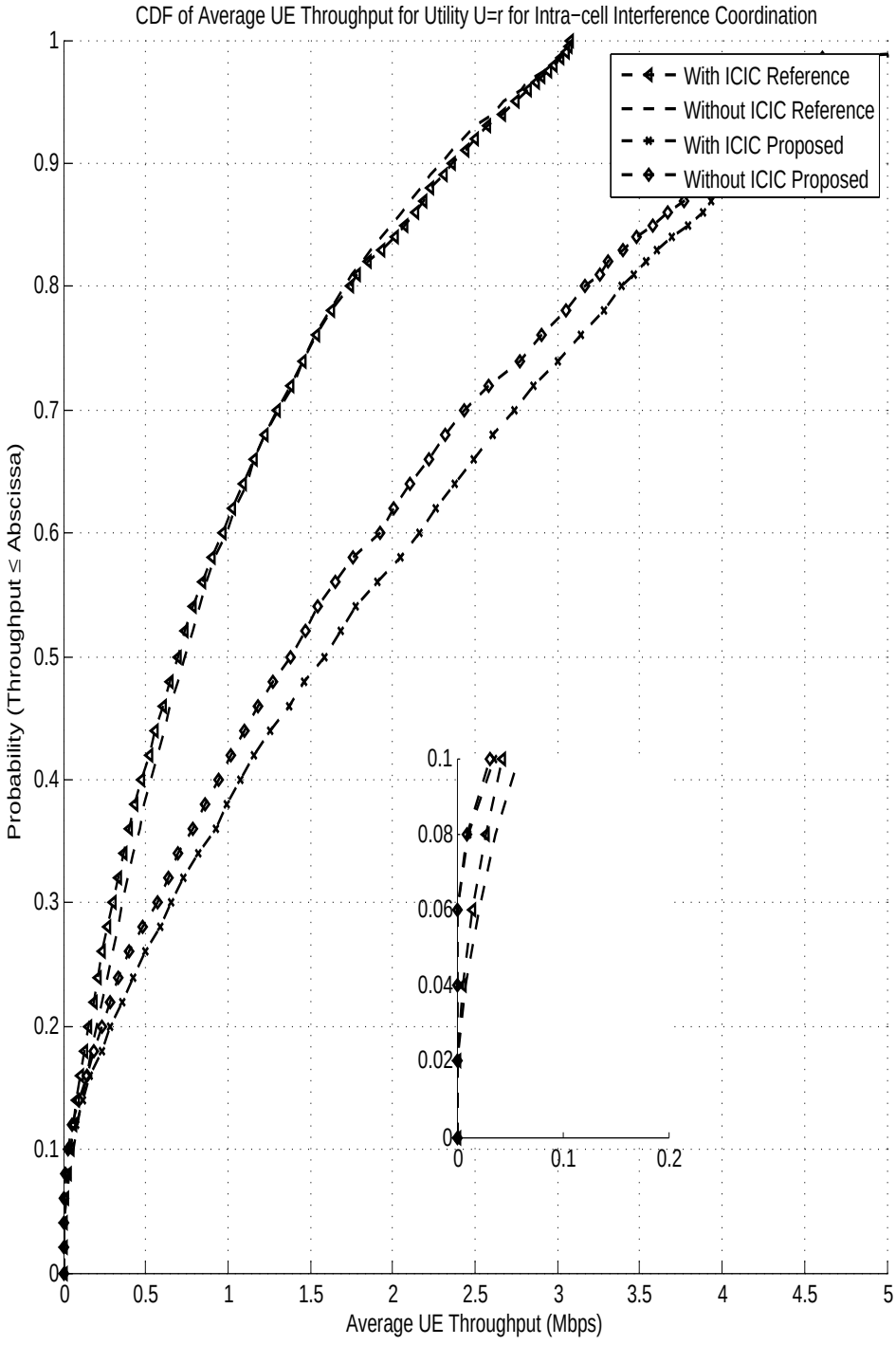

Figure 5.5: CDF of average UE throughput for intra-cell interference coordination for $U = r$

2. Sector cell-edge and total cell-edge throughput

   In table 5.7, sector cell-edge and total cell-edge throughput are given. The most noticeable values in Table 5.7 are the zero for the cell-edge spectral efficiency. The utility $U = r$ aims to maximize the overall cell-throughput which overlooks the cell-edge users in RB allocation due to their poor contribution to the total throughput. From the zoomed tail of the CDF of the Figure 5.4 and Figure 5.5, we can observe the 5th percentile point for inter-cell and intra-cell schemes, respectively.

Version	Sector Cell-Edge Throughput (kbps)	Total Cell-Edge Throughput (kbps))
Reference Scheme	13.46 (11.73)	40.40 (35.19)
Inter-cell Coordination	0 (0)	0 (0)
Intra-cell Coordination	0 (0)	0 (0)

Table 5.7: Sector cell-edge and total cell-edge throughput for $U = r$. Values in brackets correspond to no ICIC at all.

3. Cell and Cell-Edge Spectral Efficiency:

   In Table 5.8, sector and cell spectral efficiency are given. It is observed that inter-cell coordination has the best overall cell spectral efficiency. For the three schemes, performance of ICIC schemes fare better than no ICIC at all.

4. Percentage of RB utilization

   RB percentage of utilization across a cell is given in Table 5.9. The reference scheme sees the highest amount of utilization compared to the other schemes. As expected the maximum utilization for intra-cell interference for all utilities

Version	Cell Spectral Efficiency(bps/Hz)	Cell-Edge Spectral Efficiency (bps/Hz)
Reference Scheme	4.60 (4.10)	0.0040 (0.0035)
Inter-cell Coordination	14.2 (12.60)	0.00 (0.00)
Intra-cell Coordination	6.667 (6.10)	0.00 (0.00)

Table 5.8: Cell and cell-edge spectral efficiency for $U = r$. Values in brackets correspond to no ICIC at all.

was 25 percent. We observe that for the reference schemes that RB utilization always exceeds or equal to that of the ICIC which falls in line with the fact that ICIC restricts RBs from use.

Version	Resource Block Utilization
Reference Scheme	67.97 (75.32)
Inter-cell Coordination	67.47 (68.24)
Intra-cell Coordination	24.05 (24.03)

Table 5.9: Percentage of RB utilization for $U = r$. Values in brackets correspond to no ICIC at all.

5.3.3 Utility $U = rd^2$

For the utility $U = rd^2$, the CDF plots of UE throughput for both inter-cell and intra-cell interference coordination which are given by Figures 5.4 and 5.5, respectively. The performance statistics computed are further discussed next.

Figures 5.6 and 5.7 display the CDF of UE throughput for both inter-cell interference coordination and intra-cell interference coordination for $U = rd^2$, respectively. For utility $U = rd^2$, the most fair oriented scheme, we observe a reduction in overall cell throughput compared with the other utilities. The cell throughput follows the same pattern as utility $U = r$ and $U = rd$, as we observe the overall cell throughput is almost 3 times and almost 1.5 times the reference scheme for inter-cell and intra-cell interference coordination.

Performance Indicators:

1. Sector and Cell UE throughput:

   In Table 5.10, sector and cell UE throughput are given. Once again, the cell throughput compared to the reference scheme is almost thrice improved for inter-cell coordination. For intra-cell coordination cell throughput improvement is almost 1.5 times the reference scheme.

Version	Sector Throughput (Mbps)	Total Cell Throughput (Mbps)
Reference Scheme	13.50 (13.33)	40.50 (39.99)
Inter-cell Coordination	9.75 (9.87)	117.05 (118.53)
Intra-cell Coordination	4.59 (4.44)	55.08 (53.28)

Table 5.10: Sector and cell throughput for $U = rd^2$. Values in brackets correspond to no ICIC at all.

2. Sector cell-edge and total cell-edge throughput

Version	Cell-Edge Throughput (kbps)	Total Cell-Edge Throughput (kbps)
Reference Scheme	65.85 (26.21)	197.56 (78.64)
Inter-cell Coordination	21.89 (0)	262.72 (0)
Intra-cell Coordination	48.16 (26.21)	577.95 (78.64)

Table 5.11: sector cell-edge and total cell-edge throughput for $U = rd^2$. Values in brackets correspond to no ICIC at all.

In Table 5.11, sector cell-edge and total cell-edge throughput are given. For clarity, we have zoomed the tail of the CDF of the total throughput of the Figure 5.6 and Figure 5.7, we can observe the 5th percentile point for inter-cell and intra-cell schemes, respectively. From the results, we can conclude that the cell-edge performance has seen a significant improvement compared to the reference scheme.

3. Cell and Cell-Edge Spectral Efficiency:

   In Table 5.12, sector and cell spectral efficiency are given. Inter-cell coordination has the best cell spectral efficiency where as the best cell-edge spectral efficiency is for the intra-cell coordination.

Version	Cell Spectral Efficiency (bps/Hz)	Cell Edge Spectral Efficiency (bps/Hz)
Reference Scheme	4.05 (3.99)	0.019 (0.0078)
Inter-cell Coordination	11.71 (11.85)	0.0262 (0.00)
Intra-cell Coordination	4.82 (2.62)	0.0577 (0.0081)

Table 5.12: Cell and cell-edge spectral efficiency for $U = rd^2$. Values in brackets correspond to no ICIC at all.

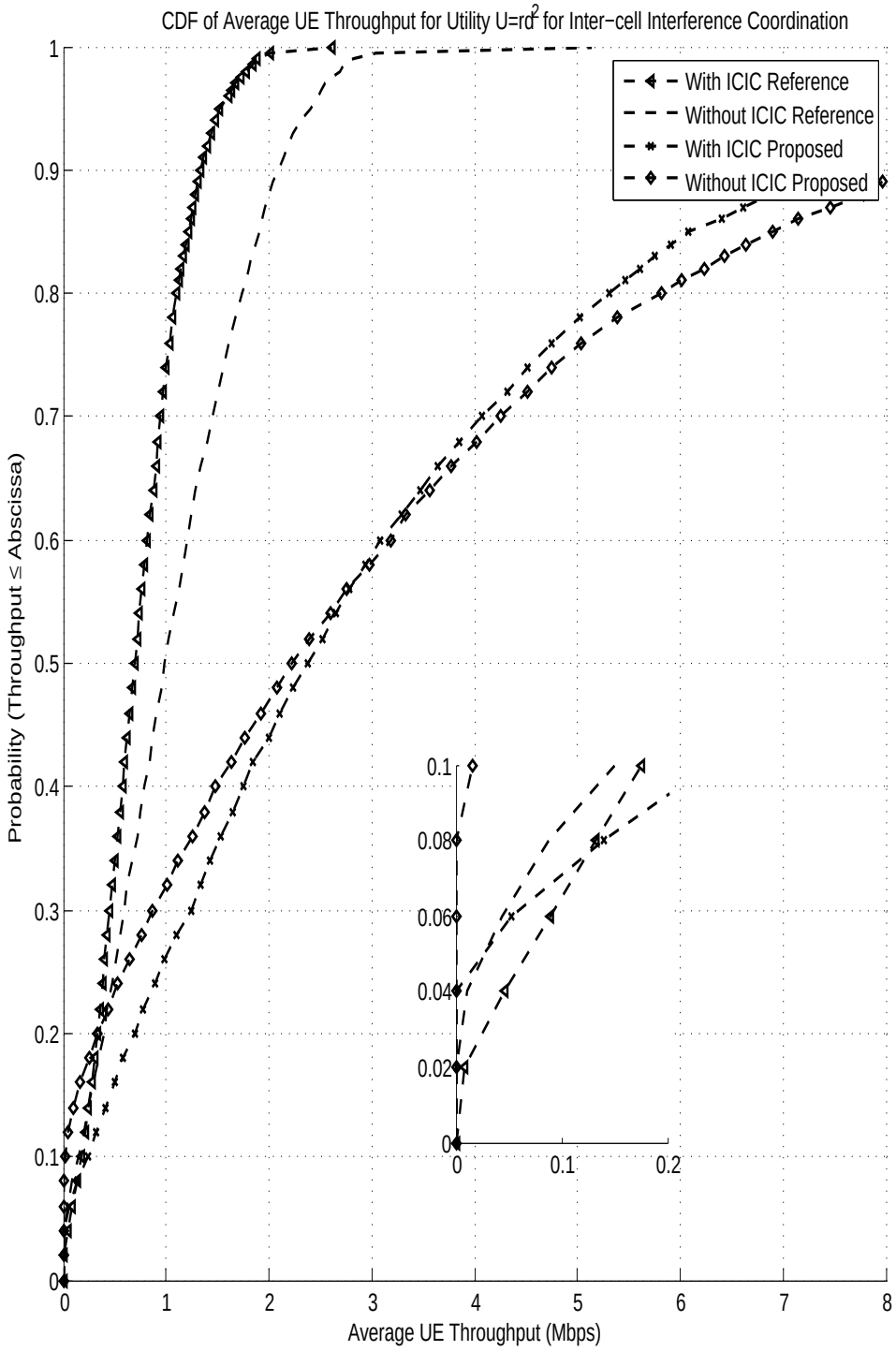

Figure 5.6: CDF of average UE througput for inter-cell interference coordination for $U = rd^2$

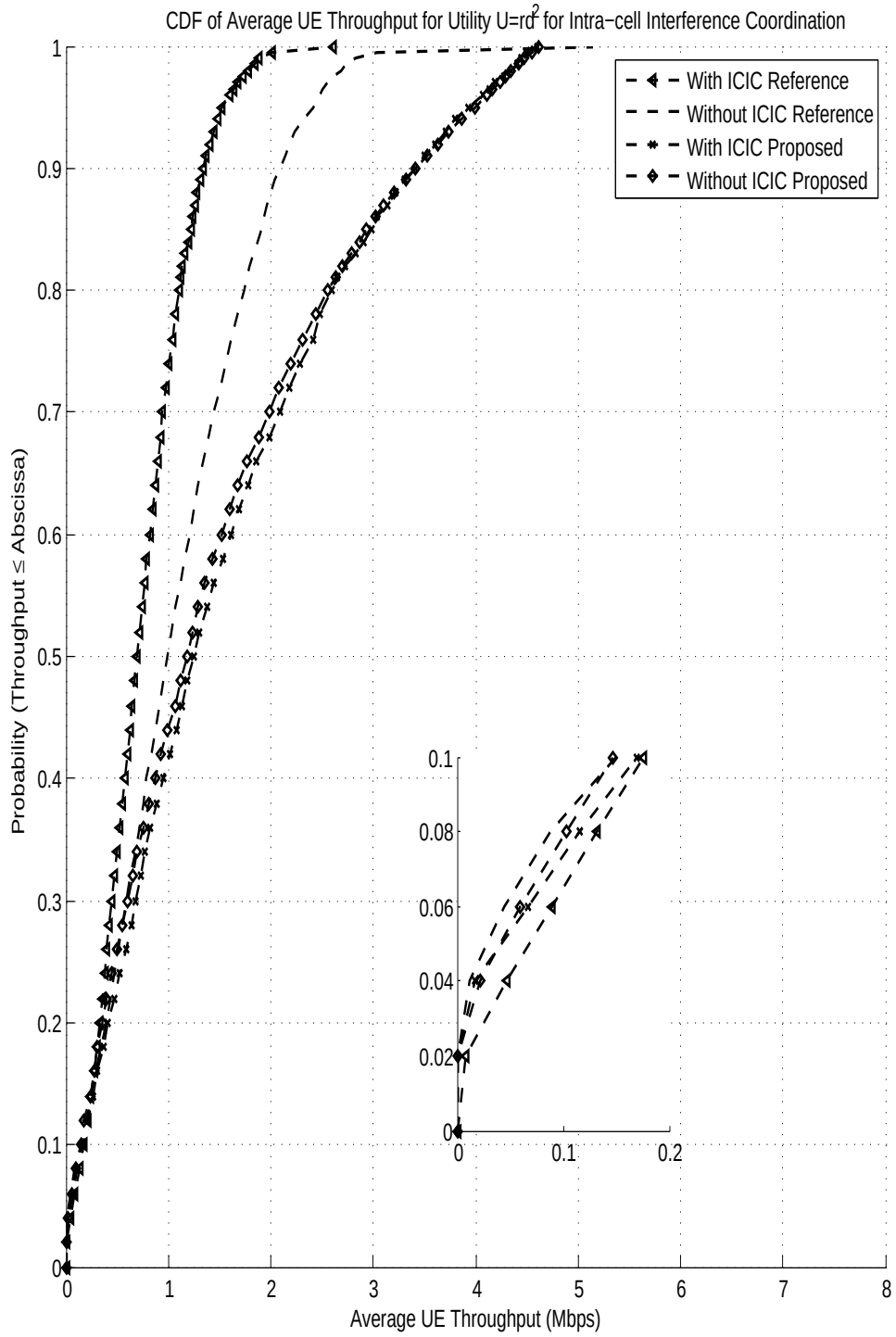

Figure 5.7: CDF of average UE througput for intra-cell interference coordination for $U = rd^2$.

4. Percentage of RB utilization

   RB percentage of utilization across a cell is given in Table 5.13. The reference scheme sees the highest amount of utilization compared to the other schemes. As expected the maximum utilization for intra-cell interference for all utilities was 25 percent. We observe that for the reference schemes that RB utilization always exceeds or equal to that of the ICIC which falls in line with the fact that ICIC restricts RBS from use.

Version	RB Utilization
Reference Scheme	76.81 (99.98)
Inter-cell Coordination	68.50 (74.86)
Intra-cell Coordination	23.98 (23.97)

Table 5.13: Percentage of RB utilization for $U = rd^2$. Values in brackets correspond to no ICIC at all.

5.4 Comparing the Three Utilities

The two schemes presented here for the three utilities, provide varying degrees of performance gains compared to the reference scheme. From one utility to another the performance gains differ, whether enhanced overall cell throughput or enhanced cell-edge throughput. An overall comparison of the three utilities will be outlined here.

The utility $U = r$ provides the best overall cell throughput across the three schemes which is expected as the demand factor was not included in the utility; this reflects the unfairness of the scheme. The unfairness is evident in the cell-edge throughput, which is the worst across the three utilities. On the other hand, it has the best total spectral efficiency of all the utilities.

The utility $U = rd^2$ has the best cell-edge throughput and spectral efficiency due to the higher weight given to the demand factor. The higher cell-edge performance comes at the expense of total cell throughput where $U = rd^2$ sees the worst overall throughput of the three utilities although its performance is better compared to the case with no ICIC at all.

The utility $U = rd$ provides a balanced approach to the ICIC schemes presented. The rate and demand factor are of equal weights in the utility function, thus neither the network throughput or the cell-edge throughput are overlooked. We can observe that the total cell throughput is better than $U = rd^2$ and that the cell-edge

performance is better that $U = r$.

5.5 Comparing the Three ICIC schemes

There are three schemes presented here: the reference scheme, inter-cell coordination and intra-cell coordination. A brief analysis comparing the three schemes will be presented here.

Inter-cell and intra-cell coordination schemes provide a significant enhancement to overall cell throughput (3 times) compared to the reference scheme. For the utility $U = r$, the performance of the reference scheme exceeded that of the two proposed schemes for cell-edge performance.

Inter-cell coordination provides the best overall cell throughput across all the utilities used, where the improvement was almost three times the reference scheme. Intra-cell coordination provides the best cell-edge performance (except for utility $U = r$). In terms of the RB utilization, the intra-cell scheme has the worst RB utilization with 75 % of RBs restricted from use.

A quick brief summary of the performance of the three schemes can be given as follows.

1. Total Cell Throughput

   Reference scheme $\leq$ Intra-cell coordination scheme $\leq$ Inter-cell coordination scheme.

2. Total Cell-edge Throughput (ignoring $U = r$)

   Reference scheme $\leq$ Inter-cell coordination scheme$\leq$ Intra-cell coordination scheme.

3. Worst RB Restriction

   Intra-cell coordination scheme $\leq$ Inter-cell coordination scheme $\leq$ Reference scheme

5.6 Implementation Complexity

Implementing the proposed algorithm has associated complexities that need to be addressed and they are:

- **Computational complexity**

  The algorithm proposed is a centralized scheme, where the optimizer lies at the central controller (Radio Network Controller (RNC) in a 3G Systems or Mobility Management Entity (MME) in LTE). The optimizer would decide which restrictions to be imposed and which would not be. It is a network level optimization where there's a large number of variables to be considered such as: number of users, number of sectors, number of RBs..etc. The sheer number of variables makes it computationally complex.

- **Complexity associated with multi-sectored base station**

  We propose a multi-sectored base station with highly directional antennas where each antenna would cover an oblong radiation pattern of 30 degrees. This setup increases the level of interference in the system. One possible drawback to its real life implementation is the intra-site and inter-site han-

dover. A vehicle moving at high speed between sectors may have, by today's standards, handover complications.

- **Signalling overhead**

  It is assumed that all UEs know the reference signals of the neighboring first-tier sectors. This signalling exchange involved in that assumption is quite large and would be difficult to implement realistically by today's standards.

- **Simulation Time for this study**

  Simulating the proposed algorithm, due to the computational complexity described above, was very time consuming. Running the simulation for a single utility takes about 5 consecutive days on parallel machines for a single scheme.

5.7 Summary: Overall Observations

Some overall observations about the proposed and reference schemes:

1. Inter-cell and intra-cell coordination improve overall throughput compared to reference scheme by almost 3 times and 1.5 times, respectively.

2. Intra-cell coordination has the worst RB utilization, i.e., the most resource loss, compared to the reference schemes as it restricts the resource usage to a maximum of twenty-five percent.

3. Order of cell throughput performance of the reference and intra-cell and inter-

cell can be given as:

Reference scheme $\leq$ Intra-cell coordination scheme $\leq$ Inter-cell coordination scheme.

4. Total Cell-edge Throughput

   Reference scheme $\leq$ Inter-cell coordination scheme $\leq$ Intra-cell coordination scheme.

5. Worst RB Restriction

   Intra-cell coordination scheme $\leq$ Inter-cell coordination scheme $\leq$ Reference scheme

6. Increasing the weights of d in the utility function decreases the overall cell throughput but it improves the cell-edge performance.

7. There's a trade-off of increasing the total cell throughput versus including fairness in the utility function.

Chapter 6

Conclusion and Future Work

In this chapter, we highlight the key aspects of the proposed work and the conclusions drawn. Possible future work and ways to improve performance are also presented in this chapter.

6.1 Summary

In the last few years, we have seen an increase in demand on wireless data networks which consequently lead to the investment in next generation 4G networks. 4G networks aim to meet the IMT-Advanced requirements which include highly ambitious expectation in terms of latency, throughput and spectral efficiency. LTE-A is expected to meet those requirements with the use of IMT-Advanced enabling technologies.

In our work, we focus on inter-cell interference coordination which is regarded as a form CoMP. ICIC plays an important role in OFDM based 4G networks as it aims to combat the high interference levels generated by the aggressive frequency reuse in the network. ICIC is a key element to achieving the high data rates promised by the 4G networks as it creates an environment that is more robust to interference.

6.2 Contributions

We proposed an enhancement to an existing ICIC scheme. The key points of the existing and proposed scheme are defined below:

Existing Scheme [12]

- Dynamic inter-cell coordination for downlink
- Use of ILP
- Multiple utility scenarios
- Problem is decomposed into sub-problems to reduce complexity

Proposed Scheme In addition to the above four points,

- Use of 12 sectored sites to increase throughput
- Intra-cell interference coordination for downlink

The use of ICIC scheme in [12] provided cell and cell-edge improvements, compared to schemes with no ICIC at all. The use of multiple sectors per cell would greatly enhance the overall cell throughput, with the use of ICIC as a method to mitigate the interference generated.

We proposed a 12-sectored site with a frequency reuse of 1. We then build upon the existing scheme and develop an inter-cell and intra-cell coordination scheme where the aim to maximize the utility. There are a few different utilities proposed with var-

ious degrees of focus on rate and user fairness. The user demand is a measure of how hungry the user is for rate in comparison to other users. Usually users at cell-edge suffer from higher pathloss and from higher interference levels from neighboring cells are more rate deprived.

We use ILP to formulate the problem proposed. The problem formulation incorporates coordination between neighboring base stations (inter-cell) or within the own cell (intra-cell) by deciding which dominant interferers is to be restricted from use. Due to the complexity of the algorithm, it it decomposed into sub-problems and solved iteratively. Two optimization tools are used to solve the centralized assignment problem.

We found that the use of 12 sectored base station has an enormous impact on cell throughput where the improvement was three times that of the reference scheme. We also found that there's significant improvement to cell-edge performance which depends on the utility used. Though the performance gain is high, there was some bandwidth loss due to resource restriction especially with the intra-cell coordination scheme. Decomposing the problem into small sub-problems relatively reduced the complexity.

6.3 Future Work

There are numerous methods to extend this thesis and to further improve performance. Some of these include:

- While the use of a 12 sectored base station improves the performance with re-

spect to the reference schemes, each sector is transmitting individually to each user. A potential enhancement could be the use of network MIMO, where the UE would receive its signal from multiple sectors at the same time.

- In our algorithm, the UE to sector assignment is done geographically i.e. a certain UE is assigned to a beam because it falls under the beam coverage area. When taking shadowing into consideration, this is not always the best approach. UE to beam assignment using received power could be a way to enhance the algorithm.

- We assume that shadowing is uncorrelated between links which is not realistic. Inclusion of correlated shadowing could potentially improve or reflect how realistic the algorithm is.

References

[1] M. Rahman and H. Yanikomeroglu, "Enhancing cell-edge performance: a downlink dynamic interference avoidance scheme with inter-cell coordination," *IEEE Transactions on Wireless Communications*, vol. 9, no. 4, pp. 1414 –1425, April 2010.

[2] "Cisco Visual Networking Index: Global Mobile Data Traffic Forecast Update, 2010 to 2015," Feb. 2011, [Online] Available: http://www.cisco.com.

[3] D. Goldman, "The tiny cube that could cut your cell phone bill," March 2011, [Online] Available: www.money.cnn.com.

[4] E. Dahlman, S. Parkvall, J. Skold, and P. Beming, *3G Evolution- HSPA and LTE for Mobile Broadband*. 1st Edition, Academic Press, 2007.

[5] "3GPP Release 10 and Beyond: HSPA+, SAE/LTE and LTE-Advanced," Feb. 2011. [Online] Available: http://www.3gamericas.org.

[6] ITU-R, "Requirements related to technical performance for IMT-Advanced radio interfaces," 2008, [Online] Available: http://www.itu.int.

[7] S. Parkvall, A. Furuskar Andre, and E. Dahlman, "Evolution of LTE toward IMT-advanced," *IEEE Communications Magazine*, vol. 49, no. 2, pp. 84 –91, February 2011.

[8] "3GPP TR 36.814 Evolved Universal Terrestrial Radio Access (E-UTRA); Further advancements for E-UTRA physical layer aspects (Release 9)," 2011. [Online] Available: http://www.3gpp.org.

[9] R. Pabst, B. Walke, D. Schultz, P. Herhold, H. Yanikomeroglu, S. Mukherjee, H. Viswanathan, M. Lott, W. Zirwas, M. Dohler, H. Aghvami, D. Falconer, and G. Fettweis, "Relay-based deployment concepts for wireless and mobile broadband radio," *IEEE Communications Magazine*, vol. 42, no. 9, pp. 80 – 89, sept. 2004.

[10] A. Ghosh, R. Ratasuk, B. Mondal, N. Mangalvedhe, and T. Thomas, "LTE-Advanced: Next-Generation wireless broadband technology [Invited Paper]," *IEEE Wireless Communications*, vol. 17, no. 3, pp. 10 –22, June 2010.

[11] G. Boudreau, N. G. Panicker, J., R. Chang, N. Wang, and S. Vrzic, "Interference coordination and cancellation for 4G networks," *IEEE Communications Magazine*, vol. 47, no. 4, pp. 74 –81, April 2009.

[12] M. Rahman and H. Yanikomeroglu, "Inter-Cell Interference Coordination in OFDMA Networks: A Novel Approach Based on Integer Programming," in *Proc. Vehicular Technology Conference (VTC 2010-Spring)*, May 2010, pp. 1 –5.

[13] "E-UTRA and E-UTRAN Overall Description; Stage 2 (Release 8), 3GPP Technical Specification TS 36.300 V9.1.0," September 2009. [Online] Available: http://www.3gpp.org. [Online]. Available: www.3gpp.org

[14] G. Fodor, C. Koutsimanis, A. Rcz, N. Reider, A. Simonsson, and W. Mller, "Intercell Interference Coordination in OFDMA Networks and in the 3GPP Long Term Evolution System," *Journal of Communications*, vol. 4, 2009. [Online]. Available: https://www.academypublisher.com

[15] "Smart Antenna Based Interference Mitigation, WINNER II Deliverable D4.7.3," June 2007 [Online] Available: http://www.ist-winner.org. [Online]. Available: http://www.ist-winner.org.

[16] C. He, F. Liu, H. Yang, C. Chen, H. Sun, W. May, and J. Zhang, "Co-Channel Interference Mitigation in MIMO-OFDM System," in *Proc. International Conference on Wireless Communications, Networking and Mobile Computing*, September 2007, pp. 204 –208.

[17] I. Fraimis, V. Papoutsis, and S. Kotsopoulos, "A Decentralized Subchannel Allocation Scheme with Inter-Cell Interference Coordination (ICIC) for Multi-Cell OFDMA Systems," in *Proc. IEEE Global Telecommunications Conference, (GLOBECOM 2010)*, December 2010, pp. 1 –5.

[18] H. Xiao and Z. Feng, "A novel fractional frequency reuse architecture and interference coordination scheme for multi-cell ofdma networks," in *Proc. Vehicular Technology Conference (VTC 2010-Spring)*, May 2010, pp. 1 –5.

[19] T. Quek, Z. Lei, and S. Sun, "Adaptive interference coordination in multi-cell ofdma systems," in *Proc. Personal, Indoor and Mobile Radio Communications, 2009 IEEE 20th International Symposium on*, Sept. 2009, pp. 2380 –2384.

[20] J. Huang, P. Xiao, and X. Jing, "2010 IEEE 21st International Symposium on Personal, Indoor and Mobile Radio Communications Workshops (PIMRC Workshops)," September 2010, pp. 420 –423.

[21] M. Rahman and H. Yanikomeroglu, "Interference Avoidance through Dynamic Downlink OFDMA Subchannel Allocation using Intercell Coordination," in *Proc. IEEE Vehicular Technology Conference,(VTC Spring 2008)*, May 2008, pp. 1630 –1635.

[22] ——, "Multicell Downlink OFDM Subchannel Allocations Using Dynamic Intercell Coordination," in *Proc. IEEE Global Telecommunications Conference, (GLOBECOM '07)*, November 2007, pp. 5220 –5225.

[23] G. Lv, S. Zhu, and H. Hui, "A Distributed Power Allocation Algorithm with Inter-Cell Interference Coordination for Multi-Cell OFDMA Systems," in *Proc. IEEE Global Telecommunications Conference (GLOBECOM 2009)*, December 2009, pp. 1 –6.

[24] K. Dong, H. Tian, X. Li, and Q. Sun, "A Distributed Inter-Cell Interference Coordination Scheme in Downlink Multicell OFDMA Systems," in *Proc. 7th IEEE Consumer Communications and Networking Conference (CCNC)*, January 2010, pp. 1 –5.

[25] R. Chang, Z. Tao, J. Zhang, and C.-C. Kuo, "Multicell OFDMA Downlink Resource Allocation Using a Graphic Framework," *IEEE Transactions on Vehicular Technology*, vol. 58, no. 7, pp. 3494 –3507, September 2009.

[26] M. Necker, "A Graph-Based Scheme for Distributed Interference Coordination in Cellular OFDMA Networks," in *Proc. IEEE Vehicular Technology Conference, 2008. (VTC Spring 2008)*, May 2008, pp. 713 –718.

[27] P. Hosein, "Cooperative scheduling of downlink beam transmissions in a cellular network," in *Proc. IEEE GLOBECOM Workshops*, 2008, pp. 1 –5.

[28] S. Parkvall, E. Englund, A. Furuska andr, E. Dahlman, T. Jo andnsson, and A. Paravati, "LTE evolution towards IMT-advanced and commercial network performance," in *2010 IEEE International Conference on Communication Systems (ICCS)*, Nov. 2010, pp. 151 –155.

[29] "TR 25.996 V10.0.0, Spatial Channel Model for Multiple Input Multiple Output (MIMO) Simulations," March 2011. [Online] Available: http://www.3gpp.org.

[30] A. Brandao, S. Luong, M. Bennai, and J. Sydor, "Practical Aspects of Interference Management in Wireless Networks Deployment Experiences at CRC," in *Proc. 3rd International Conference on Testbeds and Research Infrastructure for the Development of Networks and Communities*, May 2007, pp. 1 –6.

[31] C.-X. Wang, X. Hong, X. Ge, X. Cheng, G. Zhang, and J. Thompson, "Cooperative MIMO channel models: A survey," *IEEE Communications Magazine*, vol. 48, no. 2, pp. 80 –87, February 2010.

[32] I. Wong and B. Evans, "Performance Bounds in OFDM Channel Prediction," in *Proc. Conference on Signals, Systems and Computers, Conference Record of the Thirty-Ninth Asilomar*, November 2005, pp. 1461 – 1465.

[33] "3GPP TR 36.942 V10.2.0 technical report technical specification group radio access network; Evolved Universal Terrestrial Radio Access (E-UTRA); radio frequency (rf) system scenarios (release 10)," 2010. [Online] Available: http://www.3gpp.org.

[34] "WINNER II Test scenarios and calibration cases issue 2," Dec. 2006, [Online] Available:http://www.ist-winner.org.

[35] L. Hentil, P. Kysti, M. Kske, M. Narandzic, and M. Alatossava, "MATLAB implementation of the WINNER Phase II Channel Model Version 1.1," December 2007. [Online]. Available: https://www.ist-winner.org/phase2model.html.

[36] J. Lofberg, "YALMIP: a toolboc for modeling and optimization in MATLAB," in *Proc. IEEE Computer-Aided Control System Design (CACSD) Conference*, Taipei, Taiwan, 2004.

[37] "TOMLAB Optimization Tool," 2009, [Online] Available: http://www.tomopt.com, version 7.2.